Astronomy
&
Astrophysics

The VLT/NaCo large program to probe the occurrence of exoplanets and brown dwarfs at wide orbits[⋆,⋆⋆]

II. Survey description, results, and performances

G. Chauvin[1], A. Vigan[2], M. Bonnefoy[3], S. Desidera[4], M. Bonavita[4], D. Mesa[4], A. Boccaletti[5], E. Buenzli[3],
J. Carson[6,3], P. Delorme[1], J. Hagelberg[7], G. Montagnier[2], C. Mordasini[3], S. P. Quanz[8], D. Segransan[7], C. Thalmann[8],
J.-L. Beuzit[1], B. Biller[3], E. Covino[9], M. Feldt[3], J. Girard[10], R. Gratton[4], T. Henning[3], M. Kasper[11], A.-M. Lagrange[1],
S. Messina[12], M. Meyer[8], D. Mouillet[1], C. Moutou[2], M. Reggiani[8], J. E. Schlieder[3], and A. Zurlo[2]

[1] UJF-Grenoble1/CNRS-INSU, Institut de Planétologie et d'Astrophysique de Grenoble UMR 5274, 38041 Grenoble, France
 e-mail: Gael.Chauvin@obs.ujf-grenoble.fr
[2] Aix-Marseille Université, CNRS, LAM (Laboratoire d'Astrophysique de Marseille) UMR 7326, 13388 Marseille, France
[3] Max-Planck Institute for Astronomy, Königstuhl 17, 69117 Heidelberg, Germany
[4] INAF – Osservatorio Astronomico di Padova, Vicolo dell Osservatorio 5, 35122 Padova, Italy
[5] LESIA, Observatoire de Paris Meudon, 5 Pl. J. Janssen, 92195 Meudon, France
[6] Department of Physics & Astronomy, College of Charleston, 58 Coming Street, Charleston, SC 29424, USA
[7] Geneva Observatory, University of Geneva, Chemin des Maillettes 51, 1290 Versoix, Switzerland
[8] Institute for Astronomy, ETH Zurich, Wolfgang-Pauli-Strasse 27, 8093 Zurich, Switzerland
[9] INAF Osservatorio Astronomico di Capodimonte via Moiarello 16, 80131 Napoli, Italy
[10] European Southern Observatory, Casilla 19001, Santiago 19, Chile
[11] European Southern Observatory, Karl Schwarzschild St, 2, 85748 Garching, Germany
[12] INAF – Catania Astrophysical Observatory, via S. So a 78, 95123 Catania, Italy

ABSTRACT

Context. Young, nearby stars are ideal targets for direct imaging searches for giant planets and brown dwarf companions. After the first-imaged planet discoveries, vast efforts have been devoted to the statistical analysis of the occurence and orbital distributions of giant planets and brown dwarf companions at wide ($\geq$5–6 AU) orbits.
Aims. In anticipation of the VLT/SPHERE planet-imager, guaranteed-time programs, we have conducted a preparatory survey of 86 stars between 2009 and 2013 to identify new faint comoving companions to ultimately analyze the occurence of giant planets and brown dwarf companions at wide (10–2000 AU) orbits around young, solar-type stars.
Methods. We used NaCo at VLT to explore the occurrence rate of giant planets and brown dwarfs between typically 0.1 and 8″. Diffraction-limited observations in *H*-band combined with angular differential imaging enabled us to reach primary star-companion brightness ratios as small as 10^{-6} at 1.5″. Repeated observations at several epochs enabled us to discriminate comoving companions from background objects.
Results. During our survey, twelve systems were resolved as new binaries, including the discovery of a new white dwarf companion to the star HD 8049. Around 34 stars, at least one companion candidate was detected in the observed field of view. More than 400 faint sources were detected; 90% of them were in four crowded fields. With the exception of HD 8049 B, we did not identify any new comoving companions. The survey also led to spatially resolved images of the thin debris disk around HD 61005 that have been published earlier. Finally, considering the survey detection limits, we derive a preliminary upper limit on the frequency of giant planets for the semi-major axes of [10, 2000] AU: typically less than 15% between 100 and 500 AU and less than 10% between 50 and 500 AU for exoplanets that are more massive than 5 $M_{\rm Jup}$ and 10 $M_{\rm Jup}$ respectively, if we consider a uniform input distribution and a confidence level of 95%.
Conclusions. The results from this survey agree with earlier programs emphasizing that massive, gas giant companions on wide orbits around solar-type stars are rare. These results will be part of a broader analysis of a total of ~210 young, solar-type stars to bring further statistical constraints for theoretical models of planetary formation and evolution.

Key words. instrumentation: adaptive optics – instrumentation: high angular resolution – methods: observational – brown dwarfs – techniques: image processing – planetary systems

---

1. Introduction

Our understanding of the origin and evolution of extrasolar planets (EPs) has drastically transformed in the last decade. Current theories favor the formation of planets within a protoplanetary disk by the accretion of solids, which build up a 10 to 15 $M_{\oplus}$

core followed by rapid agglomeration of gas (Pollack et al. 1996; Alibert et al. 2004), or by gravitational instability of the gas (Boss 1997; Stamatellos & Withworth 2008; Vorobyov 2013). Whereas physical conditions and timescales favor core accretion in the inner disk (≤10 AU), gravitational instability could be the main mechanism to form massive gaseous giants at wider separations (≥10 AU) in the earliest phase of the disk's lifetime (Boley 2009). The planets could migrate either inward, toward, or outward from the star by disk-planet interactions (Kley & Nelson 2012 and reference therein) or during planet-planet interactions (Naoz et al. 2011; Dawson & Murray-Clay 2013), which alter the original semi-major axis distribution. A wide range of potential planet masses, sizes, locations, and compositions results from this flurry of formation and evolution possibilities. A major goal for exoplanetary science in the next decade is a better understanding of these mechanisms. In this context, the role of observations is crucial in providing constraints that will help to model the diversity of exoplanetary properties. The main observables are the occurrence of EPs, the physical properties and orbital characteristics (composition, mass, radius, luminosity, distribution of mass, period, and eccentricity) but also the properties of the planetary hosts (mass, age, metallicity, lithium abundance, or multiplicity).

Brown dwarfs (BDs) were originally proposed as a distinguishable class of astrophysical objects with intermediate masses between stars and planets. Recent large infrared surveys and high contrast observations have unambiguously revealed the existence of planetary mass objects, which are isolated in the field (Zapatero-Osorio et al. 2000; Liu et al. 2013; Joergens et al. 2013) or wide companions to stars (Chauvin et al. 2005a). Their existence confirms that the formation mechanisms proposed to form stars (gravo-turbulent fragmentation, disk fragmentation, accretion-ejection or photo-erosion; see Whitworth et al. 2007; Luhman 2012 for reviews) can actually form objects down to the planetary mass regime. The details of contraction and subsequent evolution of the cores remain critical and are still under considerable debate. Episodic accretion processes can affect their physical properties (Baraffe et al. 2009). It is now undeniable that the stellar and planetary formation mechanisms overlap in the substellar regime. They can both lead to the formation of planetary mass objects, including companions to stars and BDs. Fossil traces of the formation processes should be revealed by different physical features (presence of core, composition of the atmosphere, system architecture...). Distinct statistical properties such as the occurrence, the mass, separation and eccentricity distributions, should help to identify the dominant mechanism to form substellar companions.

The main statistical constraints on exoplanets originally came from the radial velocity (RV) technique. More than 800 EPs have been now confirmed, which feature a broad range of physical (mass) and orbital (P, e) characteristics around different stellar hosts (Howard et al. 2010; Mayor et al. 2011; Wright et al. 2012; Bonfils et al. 2013). The strong bimodal aspect of the secondary-mass distribution to solar-type primaries has generally been considered the most obvious evidence of different formation mechanisms for stellar and planetary systems. The period distribution of giant exoplanets is basically made of two main features: a peak around 3 days plus an increasing frequency as a function of period (Udry & Santos 2007). The observed pile up of planets with periods around 3 days is believed to be the result of migration and final stopping mechanism. The rise of the number of planets with increasing distance from the parent star reaches up to a separation corresponding to the duration limit of most of the longest surveys (5–6 AU).

This extrapolation hints that a large population of yet undetected Jupiter-mass planets may exist beyond 5 AU, suggesting an ideal niche for the direct-imaging surveys. More recently, a plethora of transiting planetary candidates have been revealed by *Kepler* (more than 2300 candidates known today, Batalha et al. 2013), which probably corroborate how abundant telluric planets are and agrees with Doppler surveys in terms of occurrence at less than 0.25 AU (Howard et al. 2012).

Despite the success of the RV and transit techniques, the time spans explored limit the studies to the close (≤5–6 AU) EPs. Within the coming years, direct imaging represents the only viable technique for probing the existence of EPs and BD companions at large (≥5–6 AU) separations. This technique is also unique for the characterization of planetary atmospheres that are not strongly irradiated by the planetary host (Janson et al. 2010; Bowler et al. 2010; Barman et al. 2011a,b; Bonnefoy et al. 2010, 2013, 2014a,b; Konopacky et al. 2013). Young (≤500 Myr), nearby stars are very favorable targets for the direct detection of the lowest mass companions. Since the discovery of the TW Hydrae association (TWA) by Kastner et al. (1997) and Hoff et al. (1998), more than 300 young, nearby stars were identified. They are gathered in several groups (TWA, β Pictoris, Tucana-Horologium, η Cha, AB Dor, Columba, Carinae), sharing common kinematics and photometric and spectroscopic properties (see Zuckerman & Song 2004; Torres et al. 2008). With typical contrast of 10−15 magnitudes for separations beyond 1.0−2.0″ (50−100 AU for a star at 50 pc), planetary mass companions down to 1−2 Jupiter masses are potentially detectable by current imaging surveys that are very deep. The first planetary mass companions were detected at large distances (≥100 AU) and/or with small mass ratio with their primaries, indicating a probable star-like or gravitational disk instability formation mechanism (Chauvin et al. 2005b; Lafrenière et al. 2008).

The breakthrough discoveries of closer and/or lighter planetary mass companions like Fomalhaut b (<1 $M_{\rm Jup}$ at 177 AU; Kalas et al. 2008, 2013), HR 8799 bcde (10, 10, 10 and 7 $M_{\rm Jup}$ at resp. 14, 24, 38, and 68 AU; Marois et al. 2008, 2010), β Pictoris b (8 $M_{\rm Jup}$ at 8 AU; Lagrange et al. 2009), or more recently κ and b (14^{+25}_{-2} $M_{\rm Jup}$ at 55 AU; Carson et al. 2013; Bonnefoy et al. 2014b), HD 95086 b (4−5 $M_{\rm Jup}$ at 56 AU; Rameau et al. 2013a,b), and GJ 504 b ($4^{+4.5}_{-1}$ $M_{\rm Jup}$ at 43.5 AU; Kuzuhara et al. 2013) indicate that we are just initiating the characterization of the outer part of planetary systems between typically 5−100 AU. Vast efforts are now devoted to systematic searches of EPs in direct imaging with an increasing number of large scale surveys (see Table 1; nine new surveys published between 2012 and 2013). The number of targets surveyed and the detection performances will increase with the new generation of planet finders LMIRCam at LBT (Skrutskie et al. 2010), MagAO (Close et al. 2012), ScExAO at Subaru (Guyon et al. 2010), SPHERE at VLT (Beuzit et al. 2008), and GPI at Gemini (Macintosh et al. 2008) with the goal to provide better statistics on larger samples and a greater number of giant planets to be characterized. It should enable the testing of alternative mechanisms to the standard planetary formation theories of core accretion and gravitation instability such as pebble accretion (Lambrechts & Johansen 2012; Morbidelli & Nesvorny 2012) or tidal downsizing (Boley et al. 2010; Nayakshin 2010; Forgan & Rice 2013) that are currently proposed to explain the existence of a population of giant planets at wide orbits. In the context of the VLT/SPHERE scientific preparation, we have conducted a large observing program (ESO: 184.C-0157) of 86 stars with NaCo

Table 1. Deep imaging surveys of young (<100 Myr) and intermediate-old to old (0.1−5 Gyr), close (<100 pc) stars that are dedicated to the search for planetary mass companions.

Reference	Telescope	Instr.	Mode	Filter	FoV (″×″)	#	SpT	Age (Myr)
Chauvin et al. (2003)	ESO3.6m	ADONIS	Cor-I	H, K	13 × 13	29	GKM	≲50
Neuhäuser et al. (2003)	NTT	Sharp	Sat-I	K	11 × 11	23	AFGKM	≲50
	NTT	Sofi	Sat-I	H	13 × 13	10	AFGKM	≲50
Lowrance et al. (2005)	HST	NICMOS	Cor-I	H	19 × 19	45	AFGKM	10−600
Masciadri et al. (2005)	VLT	NaCo	Sat-I	H, K	14 × 14	28	KM	≲200
Biller et al. (2007)	VLT	NaCo	SDI	H	5 × 5	45	GKM	≲300
	MMT		SDI	H	5 × 5	−	−	−
Kasper et al. (2007)	VLT	NaCo	Sat-I	L'	28 × 28	22	GKM	≲50
Lafrenière et al. (2007)	Gemini-N	NIRI	ADI	H	22 × 22	85		10−5000
Apai et al. (2008)[a]	VLT	NaCo	SDI	H	3 × 3	8	FG	12−500
Chauvin et al. (2010)	VLT	NaCo	Cor-I	H, K	28 × 28	88	BAFGKM	≲100
Heinze et al. (2010a,b)	MMT	Clio	ADI	L', M	15.5 × 12.4	54	FGK	100−5000
Janson et al. (2011)	Gemini-N	NIRI	ADI	H, K	22 × 22	15	BA	20−700
Vigan et al. (2012)	Gemini-N	NIRI	ADI	H, K	22 × 22	42	AF	10−400
	VLT	NaCo	ADI	H, K	14 × 14	−	−	−
Delorme et al. (2012)	VLT	NaCo	ADI	L'	28 × 28	16	M	≲200
Rameau et al. (2013c)	VLT	NaCo	ADI	L'	28 × 28	59	AF	≲200
Yamamoto et al. (2013)	Subaru	HiCIAO	ADI	H, K	20 × 20	20	FG	125 ± 8
Biller et al. (2013)	Gemini-S	NICI	Cor-ASDI	H	18 × 18	80	BAFGKM	≲200
Brandt et al. (2013)	Subaru	HiCIAO	ADI	H	20 × 20	63	AFGKM	≲500
Nielsen et al. (2013)	Gemini-S	NICI	Cor-ASDI	H	18 × 18	70	BA	50−500
Wahhaj et al. (2013)[a]	Gemini-S	NICI	Cor-ASDI	H	18 × 18	57	AFGKM	~100
Janson et al. (2013)[a]	Subaru	HiCIAO	ADI	H	20 × 20	50	AFGKM	≲1000

Notes. We have indicated the telescope, the instrument, the imaging mode (Cor-I: coronagraphic imaging; Sat-I; saturated imaging; I: imaging; SDI: simultaneous differential imaging; ADI: angular differential imaging; ASDI: angular and spectral differential imaging), the filters, the field of view (FoV), the number of stars observed (#), their spectral types (SpT), and ages (Age). [a] Surveys dedicated to planets around debris disk stars.

(hereafter the NaCo-LP). Combined with stars already observed in direct imaging, it represents a total of more than ~210 stars for studying the occurrence rate of giant planets and brown dwarf companions at wide (10−2000 AU) orbits. This complete analysis is detailed in a series of four papers: a description of the complete sample (Desidera et al. 2015), the NaCo-LP survey (this paper), the statistical analysis of the giant planet population (Vigan et al., in prep.), and that of the brown dwarf companion population (Reggiani et al., in prep.). We therefore report here the results of the NaCo-LP carried out between 2009 and 2013. In Sect. 2, we describe the target sample selection. In Sect. 3, we describe the details of the observing setup. In Sect. 4, the data reduction strategy and analysis are reported with the results in Sect. 5. Finally, a preliminary statistical analysis of the observed sample is presented in Sect. 6 and our main conclusions in Sect. 7.

2. Target properties

Based on a complete compilation of young, nearby stars that have been recently identified in young co-moving groups and from systematic spectroscopic surveys, we have selected a sample of stars according to their declination ($\delta \leq 25°$), their age ($\lesssim 200$ Myr), their distance ($d \lesssim 100$ pc), and their R-band brightness ($R \leq 9.5$). In addition, none of these stars had been observed in a high-contrast imaging survey before. Great care has been taken in the age selection criteria based on different youth diagnostics (isochrones, lithium abundance, Hα emission, X-ray activity, stellar rotation, chromospheric activity, and kinematics). Close visual (0.1−6.0″) and spectroscopic binaries were rejected

as they degrade the VLT/NaCo detection performances and bias the astrophysical interpretation. Among this sample, 86 stars were finally observed during the large program. The main target properties (spectral type, distance, age, H-band magnitude, galactic latitude, and proper motion) are reported in Table 2. They are also shown in Fig. 1 with the properties of the complete statistical sample used by Vigan et al. (in prep.) and Reggiani et al. (in prep.). A complete characterization of the NaCo-LP observed sample and the archive sample, particularly, with regard to the age and distance determination, is determined by Desidera et al. (2015). As can be seen from Fig. 1, the core of the NaCo-LP observed sample is mainly composed of close young (10−200 Myr) solar-type FGK stars.

3. Observations: telescope and instrument

We used the NaCo high contrast Adaptive Optics (AO) imager of the VLT-UT4. The NaCo instrument is equipped with the NAOS AO system (Rousset et al. 2002), and the near-infrared imaging camera CONICA (Lenzen et al. 2002). The observations were obtained during various observing runs spread between the end of 2009 and 2013 in visitor and service (queue-observing) modes. The summary of the observing runs is reported in Table 3. The NaCo-LP represents a total of 16.5 observing nights, 10.5 nights obtained in visitor mode and 6 nights in service.

To achieve high contrasts, we used angular differential imaging (ADI) on pupil-stabilized mode of NaCo. A classical Lyot-coronagraph with a diameter of 0.7″ was used during the first visitor run but then replaced by saturated imaging as the
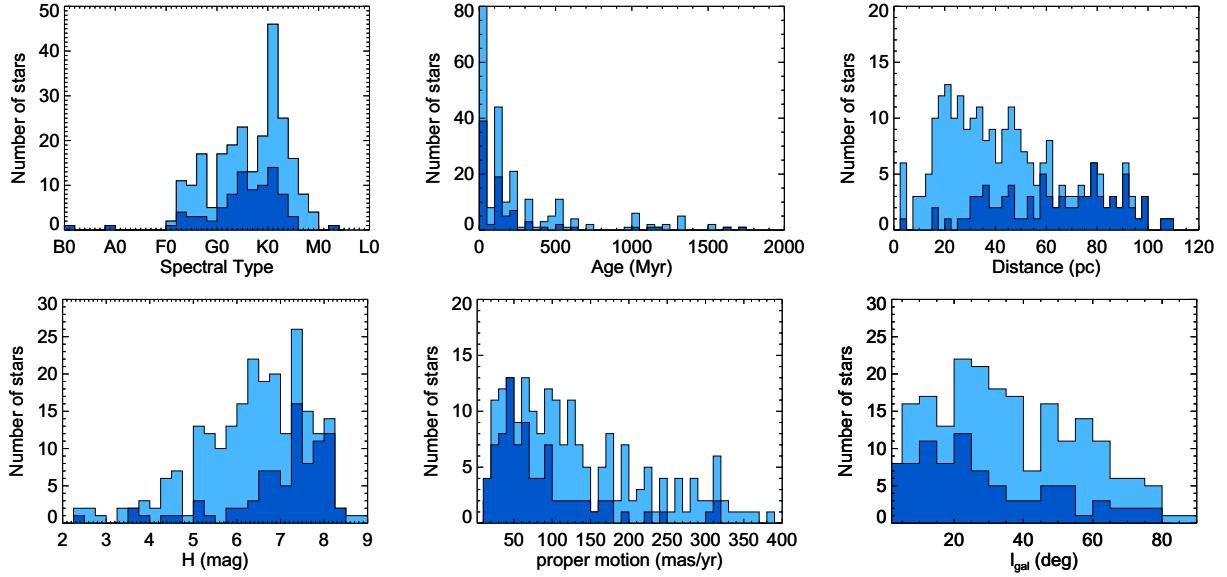
Fig. 1. Histrograms summarizing the main properties of NaCo-LP observed sample (dark blue) and of the final NaCo-LP statistical sample of ~210 stars (light blue) used by Vigan et al. (in prep.) and Reggiani et al. (in prep.): spectral type, age, distance, *H*-band magnitude, proper motion amplitude, and galactic latitude.

Table 3. Observing campaigns.

ESO Program	Mode	St. Night (UT-date)	Night (Nb)	Loss (%)	Visit (Nb)
184.C-0157A	LP-Vis	2009-11-21	3	20	23
184.C-0157E	LP-Vis	2010-02-16	3	0	27
184.C-0157B	LP-Vis	2010-06-14	2.5	70	11
184.C-0157F	LP-Vis	2010-07-29	2	33	18
184.C-0157C	LP-Ser	–	1.5	0	15
184.C-0157D	LP-Ser	–	3.3	0	33
089.C-0137A	OT-Ser	–	0.7	0	6
090.C-0252A	OT-Ser	–	0.5	0	4
Total	–	–	16.5		137

Notes. The table includes the ESO-program number, the observing mode (LP for Large-Program, OT for Open-Time, Vis for Visitor run, and Ser for Service run), the starting night, and the number of nights, the observing loss (technical and weather), and the number of observing sequences, including single and multiple visits per target.

NaCo point spread function (PSF) was unexpectedly drifting with time owing to a technical problem with the instrument. For accurate astrometry, a single observing setup was used, corresponding to the combined use of the *H*-band filter with the S13 camera (13.25 mas/pix). The time of the observations were chosen to maximize the field rotation. Typical exposure times of 1–10 s were used to saturate the PSF core by a factor 100 (a few pixels in radius) to improve the dynamic range of our images. The NaCo detector cube mode was additionally used to register each individual frame to optimize the final image selection in post-processing. The typical observing sequence was composed of a total of 10–15 cubes of 10–120 frames, which has a total integration time of 35–40 min for an observing sequence of 1–1.5 hrs on target. The parallactic angle variations are reported in Fig. 2 with the airmass, coherent energy, coherent time, as measured by NaCo, and the seeing, as measured by the DIMM seeing monitor at VLT. Non-saturated PSFs were acquired in ADI using a neutral density filter at the beginning of each observing sequence to monitor the image quality. They also

served for the calibration of the relative photometric and astrometric measurements.

4. Data reduction and analysis

4.1. Cosmetics and data processing

Three independent pipelines were used to reduce and analyze the ADI data to optimize the PSF subtraction and the detection performances and to check the consistency of the results in terms of astrometry and photometry. These pipelines are described for the LAM-ADI pipeline by Vigan et al. (2012), the IPAG-ADI pipeline by Chauvin et al. (2012), and the Padova-ADI pipeline by Esposito et al. (2013). Each pipeline processed the data in a similar way for the first cosmetic steps of flat-fielding, bad- and hot-pixel removal, and sky subtraction. To determine the central star position for the frame recentring, a Moffat fitting of the non-saturated part of the stellar PSF wing (with a similar threshold) was used. Finally, an encircled energy criteria was considered for the rejection of open-loop and poorly-corrected frames for computing a final mastercube with the corresponding parallactic angle variation. The main differences between the pipelines mostly reside in the various ADI algorithms applied (cADI and sADI, see Marois et al. 2006; LOCI, see Lafrenière et al. 2007) and in the parameters setup. Consistent results within 0.1–0.2 mag in photometry (candidate photometry and detection limits) and 0.2–0.3 pixels in astrometry were found between the different pipelines for a series of targets used as test cases. Non-saturated PSFs were similarly reduced without PSF subtraction.

The results presented in this final analysis have been obtained with the LAM-ADI pipeline using LOCI with optimization regions of $N_A = 300 \times FWHM$ at less than 3″, $N_A = 3000 \times FWHM$ at more than 3″, the radial to azimuthal width ratio $g = 1$, the radial width $\Delta r = 2 \times FWHM$, and a separation criteria of $0.75 \times FWHM$. The binning of the data was tuned to apply LOCI on a final mastercube taht is reduced to ~350 frames. An illustration of the final LOCI processed image of the young star TYC 7617-0549-1 (K0V, 76.4 pc and 30 Myr) is shown in Fig. 3.
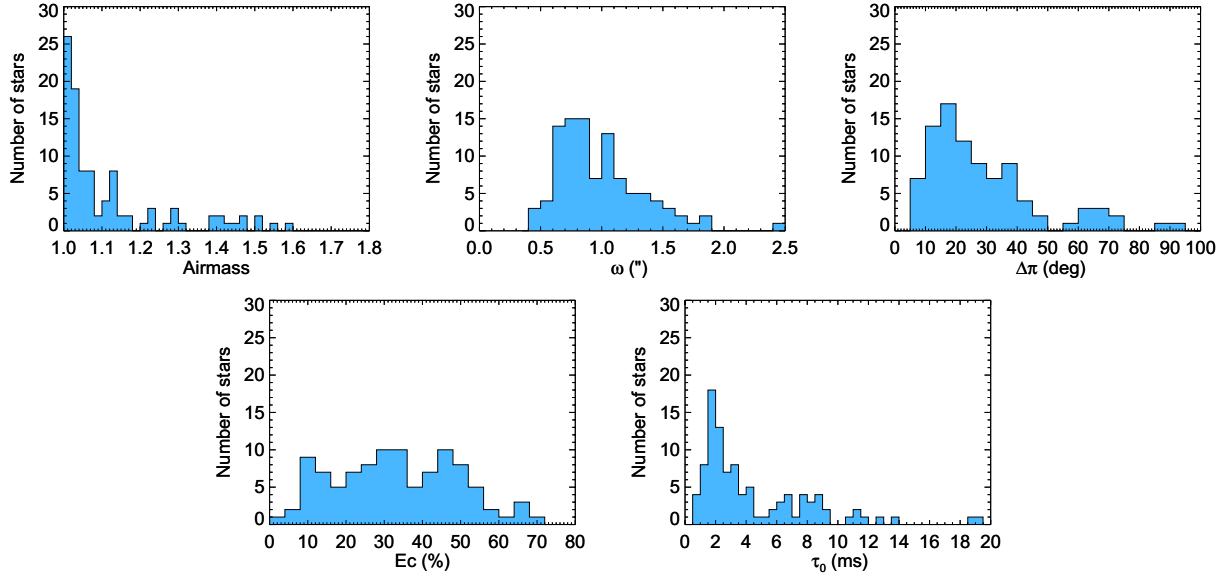
Fig. 2. Histograms summarizing the observing conditions of the NaCo-LP campaigns: airmass, DIMM seeing (ω), parallactic angle variation ($\Delta\pi$), coherent energy (Ec), and coherent time (τ_0).
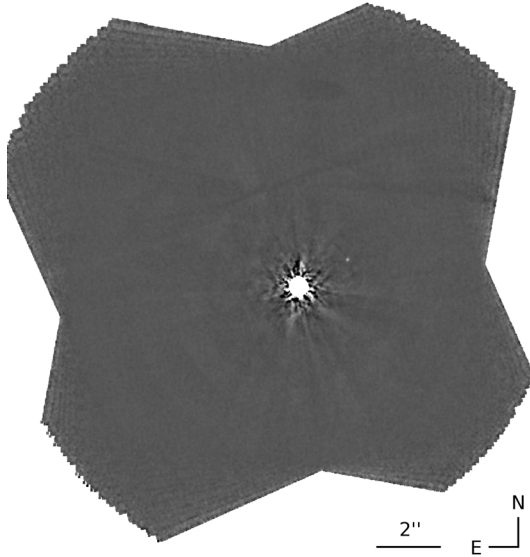
Fig. 3. VLT/NACO ADI observation in *H*-band of the young star TYC 7617-0549-1 (K0V, 76.4 pc and 30 Myr). A faint ($\Delta H = 12.7$ mag) candidate, resolved at $1.8''$, has been finally identified as a background contaminant (see Fig. 6).

4.2. Relative astrometry and photometry

The relative position and flux of all candidates was determined using Moffat fitting and aperture photometry corrected from the ADI flux loss. This first order analysis was sufficient for assessing the proper motion and nature of the candidate as described in Sect. 5.2. For the most interesting cases (like HD 8049), the injection of fake planets at the location of the candidate signal was done to properly take any local astrometric and photometric biases into account which induced by the ADI-processing described in Chauvin et al. (2012).

To finally calibrate the relative astrometric position of the detected candidates to the primary star, we used the θ_1 Ori C field observed with HST by McCaughrean & Stauffer (1994; with the same set of stars TCC058, 057, 054, 034 and 026) as a primary

Table 4. Mean plate scale and true north orientation for each observing run of the NaCo-LP.

UT Date	Platescale (mas)	True north (deg)	Calibrator
2009-11-23	13.22 ± 0.02	-0.17 ± 0.03	θ_1 Ori C
2010-02-15	13.21 ± 0.02	-0.33 ± 0.03	IDS1307
2010-02-18	13.21 ± 0.02	-0.33 ± 0.03	θ_1 Ori C
2010-06-16	13.21 ± 0.02	-0.53 ± 0.03	IDS1307
2010-07-30	13.21 ± 0.02	-0.47 ± 0.03	IDS1307
2010-12-30	13.21 ± 0.02	-0.47 ± 0.03	θ_1 Ori C
2011-01-30	13.21 ± 0.02	-0.49 ± 0.03	θ_1 Ori C
2011-05-11	13.21 ± 0.02	-0.52 ± 0.03	IDS1307
2011-07-02	13.21 ± 0.02	-0.55 ± 0.03	IDS1307
2012-01-02	13.22 ± 0.02	-0.59 ± 0.03	IDS1307
2012-01-02	13.22 ± 0.02	-0.59 ± 0.03	θ_1 Ori C

calibrator. The astrometric binary IDS 13022N0107 (van Dessel & Sinachopoulos 1993) was then used as a secondary calibrator when the θ_1 Ori C field was not observable and then recalibrated on the θ_1 Ori C field when both were observable. Both fields were observed in standard field-stabilized mode and reduced (cosmetics, flat-fielding, bad and hot-pixel removal, sky subtraction, and recentring) using the *Eclipse*[1] reduction software developed by Devillar (1997). Finally, for ADI data, the NaCo rotator offset at the start of each ADI sequence was also calibrated and taken into account as described by Chauvin et al. (2012). The results of the platescale and true north orientation determinations are given in Table 4.

The throughput of the NaCo neutral density filter was recalibrated on sky using two different datasets taken for the star TYC 9162-0698 during our February 2010 visitor run. Using aperture photometry on the data taken with and without the neutral density, we derived a transmission factor of $1.19 \pm 0.05\%$ with the *H*-band filter. This result is consistent with the one derived by Bonnefoy et al. (2013) and was used to calibrate the candidate photometry and the detection limits using the non-saturated sequence of the primary star with the neutral density filter as a photometric reference.

---

[1] http://www.eso.org/projects/aot/eclipse/
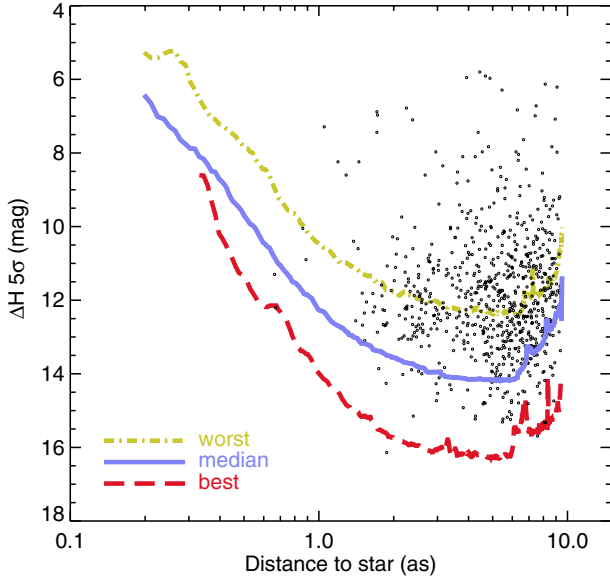
Fig. 4. VLT/NACO deep ADI 5σ detection limits in *H*-band combined with the S13 camera. The worst, median, and best detection limits are shown with all the candidates detected. Separations of less than 0.1–0.2″ are generally saturated.

4.3. Detection limit determination

A pixel-to-pixel noise map of each observation was estimated within a box of 5×5 pixels sliding from the star to the limit of the NACO field of view. To correct for the flux loss related to the ADI processing, fake planets were regularly injected for every 20 pixels in radius at 10 different position angles for separations smaller than 3″. At more than 3″, fake planets were injected for every 50 pixels at four different position angles. The final flux loss was computed with the azimuthal average of the flux losses of fake planets at the same radii. The final detection limits at 5σ were then obtained using the pixel-to-pixel noise map divided by the flux loss and normalized by the relative calibration with the primary star (considering the different exposure times and the neutral density). The LOCI processing leads to residuals whose distribution closely resembles a Gaussian (Lafrenière et al. 2007); therefore, a 5σ threshold is thus adequate for estimating detection performances. The best, worst and median detection limits of the survey are reported in Fig. 4.

5. Results

A total of 86 sources were observed. Sixteen stars were resolved as binaries, including HD 8049 with a newly discovered white dwarf companion. Ten binaries were simply observed in non-saturated ADI imaging to directly derive their relative astrometry and photometry. Seventy-six stars were observed in saturated high-contrast ADI to search for faint substellar companions. In the following sub-sections, we describe the properties of the new stellar multiple systems, the status of the detected candidates in saturated ADI, the characteristics of the white dwarf companion around HD 8049, and finally the fine analysis of the thin debris-disk around HD 61005.

5.1. New stellar close multiple systems

Despite our sample selection to reject close (0.1−6.0″) binaries, 16 stars were resolved as multiple. Three systems were already

Table 5. Relative positions and *H*-band contrast of the new binaries resolved during the NaCo-LP.

| Name	Δ (mas)	PA (deg)	ΔH (mag)
HIP 8038[a]	437 ± 7	273.8 ± 0.9	2.5 ± 0.2
HIP 80290	3340 ± 4	257.5 ± 0.2	1.9 ± 0.2
HIP 94235	506 ± 7	150.6 ± 0.8	3.8 ± 0.3
HIP 107684	326 ± 7	270.2 ± 1.2	2.8 ± 0.3
HD 199058	471 ± 7	282.9 ± 0.8	2.5 ± 0.2
TYC 0603-0461-1	74 ± 14	74.2 ± 5.1	0.1 ± 0.4
TYC 8927-3620-1[b]	87 ± 14	296.8 ± 4.35	0.5 ± 0.4
TYC 8989-0583-1	2584 ± 8	169.8 ± 0.15	2.7 ± 0.4
TYC 9010-1272-1	262 ± 8	238.0 ± 1.44	1.0 ± 0.3
TYC 9181-0466-1	1891 ± 7	123.4 ± 0.2	1.5 ± 0.2
TYC 9231-1566-1	1975 ± 7	145.5 ± 0.2	3.0 ± 0.2

Notes. Epochs of observation are reported in Table 6. [a] Known binary separated by 15.0 arcsec and $\Delta V = 2.0$ mag. [b] Third component resolved by 2MASS at ~ 4.8″ and $\Delta K = 0.7$ mag.

known, HIP 108422 AB (Chauvin et al. 2003), TYC 7835-2569-1 AB (Brandner et al. 1996), and TYC 6786-0811-1 (Köhler et al. 2000), and went through our sample selection process by mistake. The system TYC 8484-1507-1 is actually also a known ~ 8.6″ binary that was resolved by 2MASS, which is not rejected during our sample selection but resolved in the NaCo FoV, despite its large separation. Then, in the case of HD 8049, the faint comoving companion turned out to be a white dwarf. Its characteristics are briefly described in Sect. 5.3. At the end, a total of eleven new close multiple systems were resolved. All of them were observed in non-saturated ADI to derive their position and *H*-band photometry relative to the primary star (see Table 5). The visual binaries HIP 108422 AB, TYC 7835-2569-1 AB and TYC 6786-0811-1 are confirmed as physically bound. Deep ADI observations were obtained in addition to six binaries (TYC 0603-0461-1, TYC 7835-2569-1, HD 8049, TYC 8927-3620-1, HIP 80290, and TYC 8989-0583-1).

5.2. Companion candidates

Among the 76 stars observed in ADI, one companion candidate or more were detected for 43 targets (see Table 2). More than 700 candidates were detected with 90% of them in six very crowded field (see Fig. 4). The galactic contamination rate, predicted by the Besançon galactic population model (Robin et al. 2003) for the NaCo-LP fields and at least one background source, is equal to 51%, which reasonably agrees with 56% (43 systems with at least one candidate for the 76 observed). The model uses the NaCo field of view as input with the typical magnitude limit of the NaCo-LP ($H_{\rm lim} = 21$ mag) survey, and the galactic coordinates of all targets. The repartition of these galactic contaminants is given in Fig. 5. Solar-system and extra-galactic contaminants are expected to be significantly less frequent. Moreover, solar system contaminants smear during a 1 h observing sequence, and extra-galactic contaminants are mainly extended background galaxies resolved by NaCo. The most important population of contaminants that can mimic the apparent flux of the giant planet or brown dwarf companions bound to the star are M dwarfs with typical $H = 20-22$ mag apparent magnitudes.

To identify their nature, we relied on the follow-up observations at additional epochs to distinguish comoving companions from stationary background stars. The candidates were ranked
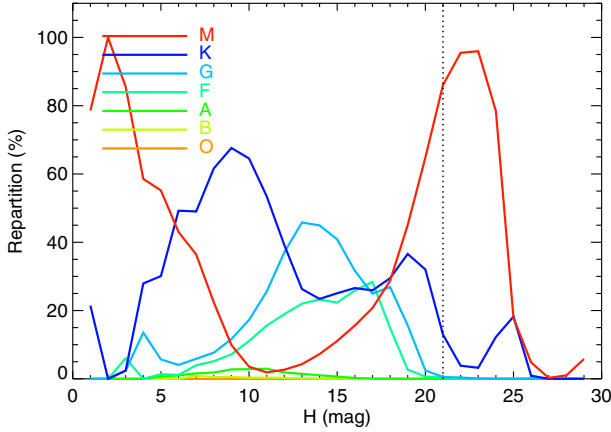
Fig. 5. Expected spectral type distribution of field stars from the Besançon galactic population model, as observed during the NaCo-LP. The FoV, the typical magnitude limit of the NaCo-LP ($H_{\mathrm{lim}} = 21$ mag), and the galactic coordinates of all targets were considered. The predicted repartion is given as a function of the spectral type and the apparent magnitude in H-band.

by priority as a function of their predicted masses (higher priority to lower masses), projected physical separations (assuming they would be bound; higher priority to closer candidates) and predicted false alarm probabilities using the Besançon galactic population model (Robin et al. 2003) to guide the follow-up strategy. Follow-up observations with a second epoch were obtained for 29 targets, including the Moth system (HD 61005) that characterized during dedicated follow-up observations. The amplitude of stellar proper motion (larger than 30 mas/yr for 80% of the NaCo-LP target) enabled a rapid identification over a 1 yr interval (see Fig. 1, bottom–middle).

For the 29 systems with at least 2-epoch observations (including the Moth system), we used a χ^2 probability test with $2 \times N_{\mathrm{epochs}}$ degrees of freedom (corresponding to the measurements: separations in the $\Delta\alpha$ and $\Delta\delta$ directions for the number N_{epochs} of epochs). This test considers the uncertainties in the relative positions measured at each epoch and the uncertainties in the primary proper motion and parallax (or distance). Figure 6 gives an illustration of a ($\Delta\alpha$, $\Delta\delta$) diagram that was used to identify a stationary background contaminant around TYC 7617-0549-1. A status has been assigned to each candidate as a background contaminant (B; $P_{\mathrm{comoving},\chi^2} < 1\%$ and with a relative motion compatible with a background source), comoving (C; $P_{\mathrm{BKG},\chi^2} < 1\%$) and with the relative motion compatible with a comoving companion), and undefined (U) when observed at only one epoch or when not satisfying the first two classifications.

Only one comoving companion, the white dwarf companion around HD 8049 described hereafter, was identified. Among the 28 other follow-up fields, ten fields have been completely characterized, and 18 are partially due to detection limits variation from one epoch to another. Fourteen fields still require second epoch observations. The status of all the candidates is given in Table 6.

5.3. A white dwarf companion around HD 8049

The only comoving companion identified in this survey with a preliminary predicted mass of 35 M_{Jup} was discovered around the star HD 8049 (K2, 33.6 pc). The star had a predicted age of 90–400 Myr from its rotational period, H&K emission and X-ray emission. Thanks to the high proper motion of the central
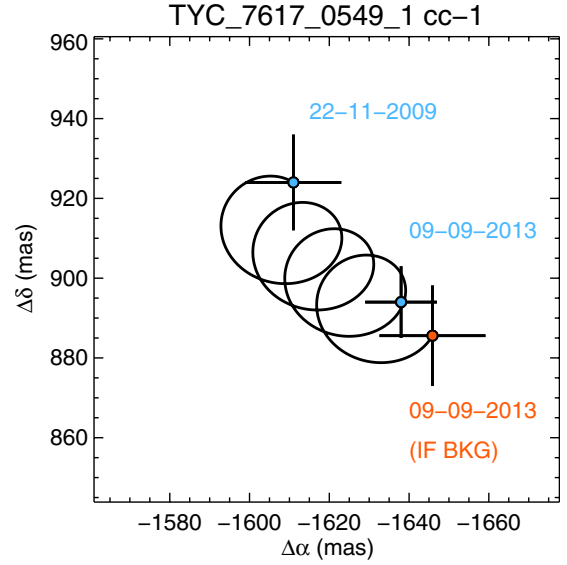
Fig. 6. VLT/NaCo measurements (filled circles with uncertainties) of the offset positions of the companion candidate to TYC 7617-0549-1 (see Fig. 3). The expected variation of offset positions, if the candidate is a background object, is shown (curved line). The variation is estimated based on the parallactic and proper motions of the primary star, as well as the initial offset position of the companion candidate from TYC 7617-0549-1. The companion candidate is clearly identified here as a stationary background contaminant.

star ($\mu_\alpha = 65.99 \pm 1.18$ mas/yr and $\mu_\delta = 240.99 \pm 0.98$ mas/yr), a χ^2 probability test on $\Delta\alpha$ and $\Delta\delta$ with respect to the star at two epochs rejected the possibility (at 99% certainty) that the object was a background source. Further analysis using archived data, radial velocity observations spanning a time range of ~30 yr, U-band imaging with EFOSC, and near-infrared spectroscopy of the comoving companion with VLT/SINFONI finally revealed that the companion was actually a white dwarf (WD) with temperature $T_{\mathrm{eff}} = 18\,800 \pm 2100$ K and mass $M_{\mathrm{WD}} = 0.56 \pm 0.08$ $M_\odot$.

This astrophysical false positive revealed that the system age was much older than initially thought. The age diagnostics have likely been affected, as the central star has been probably rejuvenated by the accretion of some amount of mass and angular momentum at the time of mass loss from the WD progenitor. A complete analysis of the system (evolution and kinematics) by Zurlo et al. (2013) actually reveals that the resulting age of the system to be about 3–6 Gyr.

5.4. The Moth resolved as a thin debris-disk

In the course of the survey, the emblematic star HD 61005 (G8V, 90 Myr, 34.5 pc), known to host The Moth debris disk (Hines et al. 2007), was observed. The NaCo H-band image remarkably resolves the disk component as a distinct narrow ring at inclination of $i = 84.3 \pm 1.0°$, with a semimajor-axis of $a = 61.25 \pm 0.85$ AU and an eccentricity of $e = 0.045 \pm 0.015$. The observations also revealed that the the ring centre is offset from the star by at least 2.75 ± 0.85 AU, which indicates a possibly dynamical perturbation by a planetary companion that perturbs the remnant planetesimal belt. The observations and the detailed disk modeling were published by Buenzli et al. (2010). Subsequent observations did not reveal any giant planet companions. Three other stars of our sample are known to host debris-disks: HIP 11360 (HD 15115; Kalas et al. 2007, Rodigas et al. 2012), HIP 99273 (HD 191089; Churcher et al. 2011), and
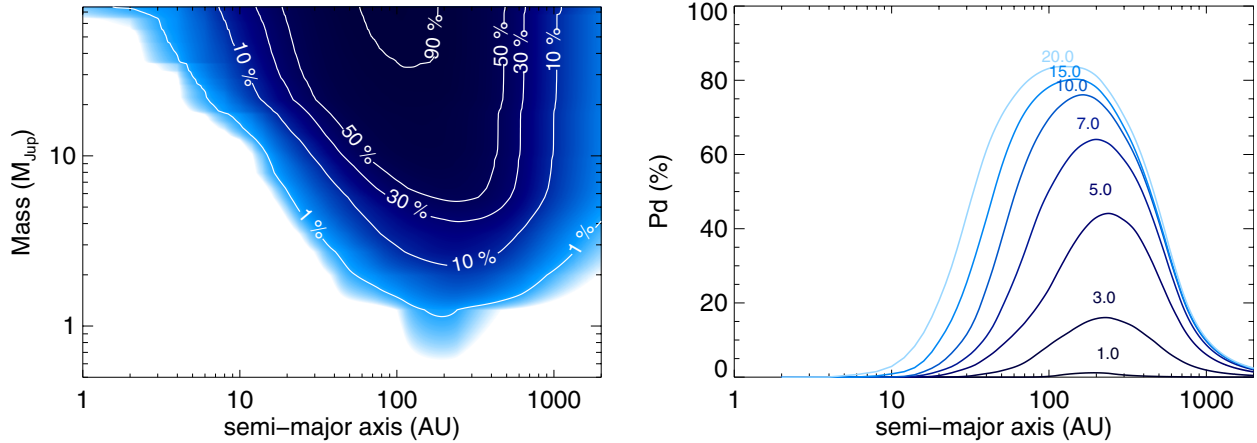
Fig. 7. *Left*: NaCo-LP mean detection probability map ($\langle p_j \rangle$) as a function of the mass and semi-major axis. *Right*: mean probability curves for different masses (1, 3, 5, 7, 10, 15, and 20 $M_{\rm Jup}$) as a function of the semi-major axis.

HIP 76829 (HD 139664; Kalas et al. 2006). No clear detection was obtained with our ADI analysis.

6. Statistical analysis

6.1. Sample definition

To define a meaningful sample for the statistical analysis of the survey, we first removed all visual and spectroscopic binaries from the sample of 76 stars observed in ADI. It includes the six visual multiple systems observed in that mode (TYC 0603-0461-1, TYC 7835-2569-1, HD 8049, HIP 8290, TYC 8927-3620-1 and TYC 8989-0583-1), and seven new spectroscopic binaries unknown at the time of our sample selection. We have then selected two sub-samples:

– the *full-stat* sample of 63 stars that includes all single stars observed in ADI with detection sensitivities down to planetary masses for physical separations ranging from 10 to 2000 AU. The status of all the candidates detected in these fields have, however, not been fully completed, although a large majority are expected to be stationary background contaminants. This sample gives an estimation of the ultimate performances of the survey in terms of masses and physical separations, when the candidate status identification will be complete, which is probably with SPHERE in the forthcoming years;

– the *complete-stat* sample of 51 stars has been restrained to all systems for which the candidate status identification up to 300 AU was complete. This includes cases with no companion candidates detected or with companion candidates properly identified thanks to our follow-up observations as stationary background sources or comoving companions. In the case of follow-up observations with variable detection performances from one epoch to another (therefore with possible undefined faint sources due to the lack of redetection), only the worst detection limit was considered. These selection criteria offered us a meaningful sample at the end for which the detection and the status identification of the candidates was complete.
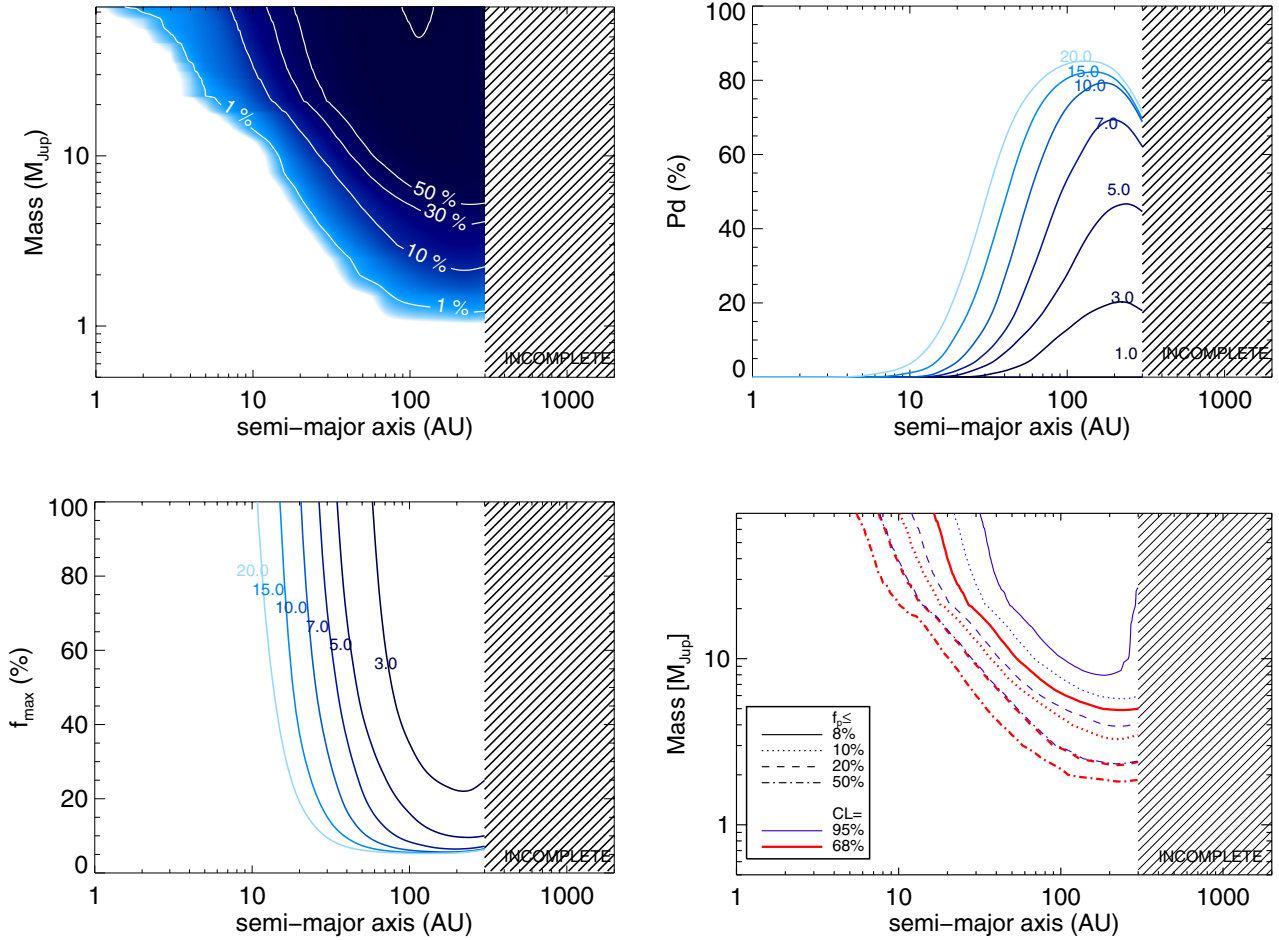
6.2. Survey detection probability

To correct for the projection effect from the observations, we then ran a set of Monte-Carlo simulations using an optimized version of the MESS code (Bonavita et al. 2012). For the *full-stat* sample, the code generates a uniform grid of mass (with a sampling of 0.5 $M_{\rm Jup}$ in the [1, 75] $M_{\rm Jup}$ interval), and semi-major axis (with a sampling of 1 AU between 1 and 1000 AU, and 2 AU between 1000 and 2000 AU for the [1, 2000] AU interval). For the *complete-stat* sample, the uniform grid is generated in the semi-major axis ranges between [1, 300] AU with a sampling of 1 AU. For each point in the grid, 100 orbits were generated and randomly oriented in space from uniform distributions in $\sin(i)$, ω, Ω, $e \leq 0.8$, and $T_{\rm p}$. The on-sky projected position (separation and position angle) at the time of the observation is then computed for each orbit and compared to our 5σ 2D-detection maps to determine the individual detection probability (p_j) of planets around each star. The average of all individual detection limits gives us the typical mean detection probability ($\langle p_j \rangle$) of the NaCo-LP to the planet and BD companion population. The results for the *full-stat* and *complete-stat* samples are shown in Figs. 7 and 8 top) respectively. The detection probabilities in both cases do not significantly differ at less than 300 AU. Most companions more massive than 20 $M_{\rm Jup}$ with a semi-major axis between 70 and 200 AU should have been detected during our survey. We are 50% sensitive to massive ($\geq$10 $M_{\rm Jup}$) planets and brown dwarfs with a semi-major axis between 60 and 400 AU. Finally, the detection of giant planets as light as 5 $M_{\rm Jup}$ between 50–800 AU is only possible for 10% of the stars observed. The relatively small number of very young stars (see Fig. 1) is responsible for this limited sensitivity to light giant planets.

6.3. Giant planet occurrence at wide orbits

To derive the occurrence of giant planets and brown dwarfs in our survey, we only considered the *complete-stat* sample with a complete census of the candidates status within 300 AU. As no planetary mass or brown dwarf companions were detected, we considered here a null-detection result. We then used the mean detection probability ($\langle p_j \rangle$) to derive the giant planet and brown dwarf occurrence upper limit ($f_{\rm max}$) that is compatible with the survey detection limits. The probability of planet detection for a survey of N stars is described by a binomial distribution, given a success probability $f p_j$ with f as the fraction of stars with planets. The parameter p_j is the individual detection probability of detecting a planet if it is present around the star j and computed previously. Assuming that the number of expected detected planets is small compared to the number of stars observed, the binomial distribution can be approximated by a Poisson distribution

Fig. 8. Results for the *complete-stat* sample. *Top left*: NaCo-LP mean detection probability map ($\langle p_j \rangle$) as a function of the mass and semi-major axis. *Top right*: mean probability curves for different masses (1, 3, 5, 7, 10, 15, and 20 $M_{\rm Jup}$) as a function of the semi-major axis. *Bottom left*: giant planet and brown dwarf occurrence upper limit ($f_{\rm max}$), considering a 95% confidence level, for different masses (3, 5, 7, 10, 15, and 20 $M_{\rm Jup}$) as a function of the semi-major axis considering the null-detection result and an uniform distribution of planets and brown dwarfs in terms of masses and semi-major axis. *Bottom right*: same occurrence upper limit ($f_{\rm max}$) expressed this time in a mass versus semi-major axis diagramme for a 68% and 95% confidence level (following Biller et al. 2007; Nielsen et al. 2008 representation).

to derive a simple analytical solution for the exoplanet fraction upper limit ($f_{\rm max}$). The formalism is described by Carson et al. (2006) and Lafrenière et al. (2007). The result is shown in Fig. 8 (bottom-left and bottom-bight). For this *complete-stat* sample, we constrain the occurrence of exoplanets that are more massive than 5 $M_{\rm Jup}$ to typically less than 15% between 100 and 300 AU. The occurence is less than 10% between 50 and 300 AU for exoplanets that are more massive than 10 $M_{\rm Jup}$. We consider here a uniform input distribution with a confidence level of 95%. These values are consistent with current estimations from various studies with comparable sensitivities around young, solar-type stars ($f_{\rm max} \leq 9.7\%$ for [0.5, 13] $M_{\rm Jup}$ planet between [50−250] AU by Lafrenière et al. 2007; $f_{\rm max} \leq 10\%$ for [1, 13] $M_{\rm Jup}$ planet between [40−150] AU by Chauvin et al. 2010; $f_{\rm max} \leq 6\%$ for [1, 20] $M_{\rm Jup}$ planet between [10−150] AU by Biller et al. 2013).

A more complete analysis, which combines the results of the NaCo-LP with archive data for a total of ~210 observed stars in direct imaging, will be presented in related papers by Vigan et al. (in prep.) and Reggiani et al. (in prep.). This analysis will provide significant and relevant statistical constraints on the population of planets and brown dwarfs around young, nearby solar-type (FGK) stars (single or members of wide binaries) and enable tests of planet and brown dwarf formation models.

7. Conclusion

In the context of the scientific preparation of the VLT/SPHERE guaranteed time, we have conducted a survey of 86 young, close and mostly solar-type stars by using NaCo at the VLT between 2009 and 2013. Our main goals were to detect new giant planets and brown dwarf companions and to initiate a relevant statistical study of their occurrence at wide (10−2000 AU) orbits. The NaCo instrument was used in pupil-stabilized mode to perform angular differential imaging at *H*-band. It enables us to reach contrast performances as small as 10^{-6} at 1.5″. Of the 86 stars observed, the survey led to

- the discovery of 11 new close binaries that we characterized in terms of relative photometry and astrometry;
- the detection of more than 700 companion candidates with 90% of them being located in six crowded fields. Among the 76 stars observed in deep ADI, 33 systems have no point-source detected in their vicinity, and 43 systems have at least one companion candidate detected. Repeated observations at several epochs enabled us to analyze the candidate status, either completely or partially, around 29 stars. Planetary mass candidates with proper follow-up were all

identified as background sources. Additional follow-up observations are still necessary to fully complete the status identification of all candidates detected in the survey owing to the variability of the detection performances from one run to another. It shows that more than two epochs are generally necessary during a survey for a full exploration of the companions content.

- The discovery of a unique comoving companion to the star HD 8049. This result has been published by Zurlo et al. (2013) and has revealed that the companion was actually a white dwarf with temperature $T_{eff} = 18\,800 \pm 2100$ K and mass $M_{WD} = 0.56 \pm 0.08\ M_{\odot}$.

- New high-contrast images of the Moth debris-disk at HD 61005. The NaCo H-band image remarkably resolves the disk component as a distinct narrow ring offset from the star by at least 2.75 ± 0.85 AU, which indicates a possibly dynamical perturbation by a planetary companion. This study was published by Buenzli et al. (2010).

- Finally, a preliminary statistical analysis of the survey detection probabitlities around the sample of 63 young, single and mostly solar-type (FGK) stars observed in angular differential imaging with detection performances enabling the search for planets and brown dwarfs in the stellar environment. Most companions that are more massive than 20 M_{Jup} with a semi-major axis between 70 and 200 AU should have been detected during our survey. We are 50% sensitive to massive ($\geq 10\ M_{Jup}$) planets and brown dwarfs with a semi-major axis between 60 and 400 AU. Finally, the detection of giant planets as light as 5 M_{Jup} between 50–800 AU is only possible for 10% of the stars observed. We have then defined a more complete sample of 51 stars restrained to all systems for which the candidate status identification was complete up to 300 AU. This includes cases with no companion candidates detected or with companion candidates properly and completely identified. Based on this complete sample average detection probability, a non-detection result, and the consideration of a uniform distribution of giant planets and brown dwarf companions in terms of semi-major axis and mass, we derive a typical upper limit for the occurrence of exoplanets that are more massive than 5 M_{Jup} of 15% between 100 and 300 AU, and a limit of 10% between 50 and 300 AU for EPs that are more massive than 10 M_{Jup} with a confidence level of 95%.

Combined with compiled archived data, the results of this survey offer a unique sample of ~210 young, solar-type stars that are observed in deep imaging as a mean to constrain the presence of giant planets and brown dwarfs in their close environment. A more complete statistical analysis will be published in two linked articles by Vigan et al. (in prep.) and Reggiani et al. (in prep.), which will test the relevance of various analytical distributions for describing the giant planet and brown dwarf companion population at wide orbits but will also bring further constraints on current theories of planetary formation. All final products of this survey (images, detection limits, and candidate status) will be released in the Deep Imaging Virtual Archive (DIVA) database with the archive data used for full statistical analysis. We encourage the community to support this effort by sharing the final products (reduced images, detection limits, and candidate relative astrometry, photometry, and status) of their published surveys to optimally prepare the future of planet imaging searches that come with the new generation of planet imagers like LMIRCam, MagAO, SPHERE, GPI, and SCExAO. In the long term, these include JWST (Clampin 2010), TMT-PFI

(Simard et al. 2010), and the EELT instruments (METIS or E-MIDIR, Brandl et al. 2010; EPICS or E-PCS, Kasper et al. 2010).

References

Alibert, Y., Mordasini, C., & Benz, W. 2004, A&A, 417, L25
Apai, D., Janson, M., Moro-Martín, A., et al. 2008, ApJ, 672, 1196
Baraffe, I., Chabrier, G., & Gallardo, J. 2009, A&A, 702, 27
Barman, T. S., Macintosh, B., Konopacky, Q. M., & Marois, C. 2011a, ApJ, 733, 65
Barman, T. S., Macintosh, B., Konopacky, Q. M., & Marois, C. 2011b, ApJ, 735, L39
Batalha, N. M., Rowe, J. F., Bryson, S. T., et al. 2013, ApJS, 204, 24
Beuzit, J.-L., Feldt, M., Dohlen, K., et al. 2008, SPIE, 7014, 41
Biller, B. A., Close, L. M., Masciadri, E., et al. 2007, ApJS, 173, 143
Biller, E., Liu, M., Wahhaj, Z., et al. 2013, ApJ, 777, 160
Boley, A. C. 2009, ApJ, 695, L53
Boley, A. C., Hayfield, T., Mayer, L., & Durisen, R. H. 2010, Icarus, 207, 509
Bonavita, M., Chauvin, G., Desidera, S., et al. 2012, A&A, 537, A67
Bonfils, X., Delfosse, X., Udry, S., et al. 2013, A&A, 549, A109
Bonnefoy, M., Chauvin, G., Lagrange, A. M., et al. 2010, A&A, 512, A52
Bonnefoy, M., Boccaletti, A., Lagrange, A. M., et al. 2013, A&A, 555, A107
Bonnefoy, M., Chauvin G., Lagrange, A. M., et al. 2014a, A&A, 562, A127
Bonnefoy, M., Currie, M., Marleau, G. D., et al. 2014b, A&A, 562, A111
Boss, A. P. 1997, Science, 276, 1836
Bowler, B., Liu, M., Dupuy, T. J., & Cushing, M. C. 2010, ApJ, 723, 850
Brandl, B. R., Lenzen, R., Pantin, E., et al. 2010, SPIE, 7735, 83
Brandner, W., Alcala, J. M., Kunkel, M., Moneti, A., & Zinnecker, H. 1996, A&A, 307, 121
Brandt, T., Kuzuhara, M., McElwain, M. W., et al. 2013, ApJ, 786, 1
Buenzli, E., Thalmann, C., Vigan, A., et al. 2010, A&A, 524, L1
Carson, J., Eikenberry, S. S., Smith, J. J., & Cordes, J. M. 2006, AJ, 132, 1146
Carson, J., Thalmann, C., Janson, M., et al. 2013, ApJ, 763, L32
Chauvin, G., Thomson, M., Dumas, C., et al. 2003, A&A, 404, 157
Chauvin, G., Lagrange, A.-M., Zuckerman, B., et al. 2005a, A&A, 438, L29
Chauvin, G., Lagrange, A.-M., Dumas, C., et al. 2005b, A&A, 438, L25
Chauvin, G., Lagrange, A.-M., Bonavita, M., et al. 2010, A&A, 509, A52
Chauvin, G., Lagrange, A.-M., Beust, H., et al., 2012, A&A, 542, A41
Churcher, L., Wyatt, M., & Smith, R. 2011, MNRAS, 410, 2
Clampin, M. 2010, in Pathways Towards Habitable Planets, ASP Conf. Ser., 430, 167
Close, L., Males, J. R., Kopon, D. A., et al. 2012, SPIE, 8447, 0
Delorme, P., Lagrange, A.-M., Chauvin, G., et al. 2012, A&A, 539, A72
Desidera S., Covino E., Messina S., et al. 2015, A&A, 573, A126
Devillar, N. 1997, The Messenger, 87, 19
Esposito, S., Mesa, D., Skemer, A., et al. 2013, A&A, 549, A52
Dawson, R. I., & Murray-Clay, R. A. 2013, ApJ, 767, L24
Forgan, D., & Rice, K. 2013, MNRAS, 432, 3168
Guyon, O., Martinache, F., Garrel, V., et al. 2010, SPIE, 7736, 71
Heinze, A. N., Hinz, P. M., Sivanandam, S., et al. 2010a, ApJ, 714, 1551
Heinze, A. N., Hinz, P. M., Kenworthy, M., et al. 2010b, ApJ, 714, 1570
Hines, D. C., Schneider, G., Hollenbach, D., et al. 2007, ApJ, 671, L165
Hoff, W., Henning, T., & Pfau, W. 1998, A&A, 336, 242
Howard, A. W., Johnson, J. A., & Marcy, G. W. 2010, ApJ, 721, 1467
Howard, A. W., Marcy, G. W., & Bryson, S. T. 2012, ApJ, 201, 15
Janson, M., Bergfors, C., Goto, M., Brandner, W., & Lafrenière, D. 2010, ApJ, 710, L35
Janson, M., Bonavita, M., Klahr, H., et al. 2013a, ApJ, 736, 89
Janson, M., Brandt, T. D., Moro-Martín, A., et al. 2013b, ApJ, 773, 73
Joergens, V., Bonnefoy, M., Liu, Y., et al. 2013, A&A, 558, L7
Kalas, P., Graham, J. R., Clampin, M. C., & Fitzgerald, M. P. 2006, ApJ, 637, L57

Kalas, P., Fitzgerald, M. P., & Graham, J. R. 2007, ApJ, 661, L85
Kalas, P., Graham, J. R., Chiang, E., et al. 2008, Science, 322, 1345
Kalas, P., Graham, J. R., Fitzgerald, M. P., & Clampin, M. 2013, ApJ, 775, 56
Kasper, M., Apai, D., Janson, M., & Brandner, W. 2007, A&A, 472, 321
Kasper, M., Beuzit, J.-L., Vérinaud, C., et al. 2010, SPIE, 7735, 81
Kastner, J. H., Zuckerman, B., Weintraub, D. A., & Forveille, T. 1997, Science, 277, 67
Kley, W., & Nelson, R. P. 2012, ARA&A, 50, 211
Köhler, R., Kunkel, M., Leinert, C., & Zinnecker, H. 2000, A&A, 356, 541
Konopacky, Q. M., Barman, T. S., Macintosh, B. A., & Marois, C. 2013, Science, 339, 1398
Kuzuhara, M., Tamura, M., Kudo, T., et al. 2013, ApJ, 774, 11
Lafrenière, D., Doyon, R., Marois, C., et al. 2007, ApJ, 670, 1367
Lafrenière, D., Jayawardhana, R., van Kerkwijk, M. H., et al. 2008, ApJ, 689, 153
Lagrange, A.-M., Gratadour, D., Chauvin, G., et al. 2009, A&A, 506, L972
Lambrechts, M., & Johansen, A. 2012, A&A, 544, L32
Lenzen, R., Hartung, M., Brandner, et al. 2002, SPIE, 4841
Liu, M. C., Magnier, E. A., Deacon, N. R., et al. 2013, ApJ, 777, L20
Lowrance, P. J., Becklin, E. E., Schneider, G., et al. 2005, AJ, 130, 1845
Luhman, K. 2012, ARA&A, 50, 65
Macintosh, B., Graham, J. R., Palmer, D., et al. 2008, SPIE, 7015, 31
Marois, C., Lafrenière, D., Doyon, R., Macintosh, B., & Nadeau, D. 2006, ApJ, 641, 556
Marois, C., Macintosh, B., Barman, T., et al. 2008, Science, 322, 1348
Marois, C., Zuckerman, B., Konopacky, Q. M., Macinosh, B., & Barman, T. 2010, Nature 468, 1080
Masciadri, E., Mundt, R., Henning, Th., & Alvarez, C. 2005, ApJ, 625, 1004
Mayor, M., Marmier, M., Lovis, C., et al. 2011, A&A, submitted [arXiv:1109.2497]
McCaughrean, M. J., & Stauffer, J. R. 1994, AJ, 108, 1382

Morbidelli, A., & Nesvorny, D. 2012, A&A, 546, A18
Naoz, S., Farr, W. M., Lithwick, Y., Rasio, F. A., & Teyssandier, J. 2011, Nature, 473, 187
Nayakshin, S. 2010, MNRAS, 402, 789
Neuhäuser, R., Guenther, E. W., Alves, J., et al. 2003, Astron. Nachr., 324, 535
Nielsen, E., Liu, M., Wahhaj, Z., et al. 2013, ApJ, 776, 4
Pollack, J. B., Hubickyj, O., Bodenheimer, P., et al. 1996, Icarus, 124, 62
Rameau, J., Chauvin, G., Lagrange, A.-M., et al. 2013a, ApJ, 772, L15
Rameau, J., Chauvin, G., Lagrange, A.-M., et al. 2013b, ApJ, 779, L26
Rameau, J., Chauvin, G., Lagrange, A.-M., et al. 2013c, A&A, 553, A60
Robin, A. C., Reylé, C., Derrière, S., & Picaud, S. 2003, A&A, 409, 523
Rodigas, T. J., Hinz, P. M., Leisenring, J., et al. 2012, ApJ, 752, 57
Rousset, G., Lacombe, F., Puget, P., et al. 2002, SPIE, 4007
Skrutskie, M. F., Jones, T., Hinz, P., et al. 2010, SPIE, 7735, 118
Simard, L., Crampton, D., Ellerbroek, B., & Boyer, C. 2010, SPIE, 7735, 70
Stamatellos, D., & Withworth, A. P. 2008, A&A, 480, 879
Torres, C. A. O., Quast, G. R., Melo, C. H. F., & Sterzik, M. F. 2008, in Handbook of Star Forming Regions, Vol. II: The Southern Sky ASP Monograph Publications, 5, 757
Udry, S., & Santos, N. C. 2007, ARA&A, 45, 397
van Dessel, E., & Sinachopoulos, D. 1993, A&AS, 100, 517
Vigan, A., Patience, J., Marois, C., et al. 2012, A&A, 544, A9
Vorobyov, E. I. 2013, A&A, 552, A129
Wahhaj, Z., Liu, M., Nielsen, E. L., et al. 2013, ApJ, 773, 179
Whitworth, A., Bate, M. R., Nordlund, A., Reipurth, B., & Zinnecker, H. 2007, PPV Conf. (Tucson: University of Arizona Press), 951, 459
Wright, H. S., Marcy, G. W., Howard, A. W., et al. 2012, ApJ, 753, 160
Yamamoto, K., Matsuo, T., Shibai, H., et al. 2013, PASJ, 65, 90
Zapatero Osorio, M. R., Béjar, V. J. S., & Martín, E. L. 2000, Science, 290, 103
Zuckerman, B., & Song, I. 2004, ARA&A, 42, 685
Zurlo, A., Vigan, A., Hagelberg, J., et al. 2013, A&A, 554, A21

Table 2. NaCo-LP target sample and properties.

Name-1	Name-2	H (mag)	SpT	d (pc)	Age (Myr)	Binarity	Mode	Comments
TYC 5839-0596-1	BD-16-20	6.6	K0IVe	43.5	150.	SB2	sat, ADI, H	
TYC 0603-0461-1	BD+07-85	7.4	K4Ve	58.2	100.	Bin (new)	sat, ADI, H	
HIP 3924	HD 4944	6.7	F7V	53.2	500.	SB2	sat, ADI, H	
HIP 6177	HD 8049	6.7	K2V	33.6	3000.		sat, ADI, H	cc
HIP 8038	HD 10611B	7.2	K5Ve	29.3	150.	Bin (new)	nonsat, ADI, H	
HIP 10602	HD 14228	4.0	B0V	47.1	30.		sat, ADI, H	
HIP 11360	HD 15115	5.9	F2	45.2	30.		sat, ADI, H	
TYC 8484-1507-1	CD-53-535	6.6	G8V	60.5	100.	Bin (known)	nonsat, ADI, H	
HIP 12394	HD 16978	4.4	B9III	46.6	30.		sat, ADI, H	
HIP 13008	HD 17438	5.5	F2V	39.6	1000.		sat, ADI, H	cc
HIP 14684	IS-Eri	6.8	G0	37.4	100.		sat, ADI, H	cc
TYC 8060-1673-1	CD-46-1064	7.2	K3V	40.4	30.		sat, ADI, H	
HIP 19775	HD 26980	7.7	G3V	80.5	30.		sat, ADI, H	
HIP 23316	HD 32372	7.9	G5V	76.3	30.		sat, ADI, H	
HD 32981	BD-16-1042	7.8	F8V	86.7	100.		sat, ADI, H	
BD-09-1108	xxxx	8.2	G5	93.6	30.		sat, ADI, H	
HIP 25434	HD 274197	7.9	G0	79.1	20.		sat, ADI, H	ccs
TYC 9162-0698-1	HD 269620	8.2	G6V	77.7	30.		sat, ADI, H	ccs
TYC 5346-132-1	BD-08-1195	8.1	G7	81.2	30.		sat, ADI, H	ccs
HIP 30261	HD 44748	7.6	G6V	61.8	100.		sat, ADI, H	
TYC 7617-0549-1	CD-40-2458	8.2	K0V	77.8	30.		sat, ADI, H	cc
TYC 9181-0466-1	HD 47875	7.4	G4V	77.7	30.	Bin (new)	nonsat, ADI, H	
HIP 32235	HD 49855	7.4	G6V	58.2	30.		sat, ADI, H	cc
HIP 35564	HD 57852	5.1	F2	31.7	200.	RV var	sat, ADI, H	ccs
TYC 8128-1946-1	CD-48-2972	8.1	G8V	89.7	45.		sat, ADI, H	ccs
HIP 36414	HD 59704	6.5	F7V	52.5	200.	SB, RV var	sat, ADI, H	ccs
HIP 36948	HD 61005	6.6	G5V	35.3	45.		sat, ADI, H	ccs
HIP 37563	HD 62850	5.9	G3V	32.8	200.		sat, ADI, H	
HIP 37923	HD 63608	6.5	K0V	36.8	200.		sat, ADI, H	ccs
TYC 8927-3620-1	HD 77307	7.7	G8IV	81.8	20.	Bin (new)	sat, ADI, H	
HIP 46634	BD+11-2052B	6.8	G5	42.3	300.		sat, ADI, H	
HIP 47646	HD 84199	6.9	F5V	73.6	1150.		sat, ADI, H	
TWA-21	HD 298936	7.3	K3Ve	54.8	17.		sat, ADI, H	ccs
TYC 7188-0575-1	CD-31-8201	7.4	K0Ve	43.2	150.	SB2	sat, ADI, H	ccs
TYC 6069-1214-1	BD-19-3018	8.0	K0V	67.8	70.		sat, ADI, H	
TYC 7722-0207-1	HD 296790	7.8	K0V	65.8	100.		sat, ADI, H	ccs
TYC 7743-1091-1	HD 99409	5.2	G6III	200.0	1700.		sat, ADI, H	
HIP 58240	HD 103742	6.2	G3V	31.8	200.		sat, ADI, H	cc
TYC 9231-1566-1	HD 105923	7.3	G8V	96.0	10.	Bin (new)	nonsat, ADI, H	
TYC 8979-1683-1	CD-62-657	7.5	G7V	75.6	17.		sat, ADI, H	ccs
TYC 8989-0583-1	HD 112245	7.4	K0Ve	65.4	17.	Bin (new)	sat, ADI, H	
TYC 9245-0617-1	CD-69-1055	7.7	K0Ve	93.0	10.		sat, ADI, H	ccs
HIP 63862	HD 113553	6.8	G5V	49.0	150.		sat, ADI, H	ccs
TYC 7796-2110-1	CD-41-7947	8.3	K2IVe	92.1	17.		sat, ADI, H	ccs
TYC 9010-1272-1	HD 124831	7.8	G3V	86.5	30.	Bin (new)	nonsat, ADI, H	
HIP 70351	HD 125485	7.6	G7V	91.7	110.		sat, ADI, H	ccs
HIP 71908	GJ-560A	2.5	F1V	16.6	1110.		sat, ADI, H	cc
HIP 71933	HD 129181	7.2	F8V	83.9	16.		sat, ADI, H	ccs
HIP 72399	HD 130260A	7.5	K3Ve	46.1	500.	SB1, RV var	sat, ADI, H	
TYC 7835-2569-1	HD 137059	7.1	G3V	70.2	120.	SB2 + Bin (known)	sat, ADI, H	
HIP 76829	HD 139664	3.7	F5IV	17.4	200.		sat, ADI, H	ccs
TYC 6781-0415-1	CD-24-12231	7.4	G9IVe	106.0	11.		sat, ADI, H	
TYC 6786-0811-1	CD-27-10549	7.5	K0IV	78.6	60.	Bin (known)	nonsat, ADI, H	
HIP 78747	HD 143928	5.1	F3V	37.9	1600.		sat, ADI, H	ccs
TYC 6209-0769-1	BD-19-4341	7.4	K0IV	43.9	120.		sat, ADI, H	cc
HIP 79958	HD 146464	6.7	K3Ve	27.2	130.		sat, ADI, H	ccs
HIP 80290	HD 147491	8.0	G2IV	83.3	30.	Bin (new)	sat, ADI, H	ccs
HIP 80758	HD 148440	8.0	G9Ve	98.2	20.		sat, ADI, H	ccs

Notes. In addition to the target name, *H*-band magnitude, spectral type, distance, and age, we have reported the multiplicity status with a flag (Bin for visual binaries with the indication that they are new or known, SB for spectroscopic binaries, RV var for radial velocity variable), the observing mode (nonsat for non-saturated or sat for saturated, ADI for angular differential imaging and the filter) and the presence of companion candidates (ccs).

Table 2. continued.

Name-1	Name-2	H (mag)	SpT	d (pc)	Age (Myr)	Binarity	Mode	Comments
TYC 6818-1336-1	HD 153439	7.8	G0IV	89.5	30.		sat, ADI, H	ccs
TYC 6815-0084-1	CD-25-11942	7.7	K0IV	92.0	11.		sat, ADI, H	ccs
TYC 6815-0874-1	CD-25-11922	10.1	G2IV	109.0	20	SB2?	sat, ADI, H	ccs
TYC 7362-0724-1	HD 156097	7.8	G5V	90.0	20.		sat, ADI, H	ccs
TYC 8728-2262-1	CD-54-7336	7.5	K1V	70.4	12.		sat, ADI, H	ccs
HIP 86672	HD 160682	7.4	G5V	78.0	30.		sat, ADI, H	ccs
HIP 89829	HD 168210	7.2	G5V	72.6	16.		sat, ADI, H	ccs
HIP 93375	HD 176367	7.3	G1V	58.8	100.		sat, ADI, H	ccs
HIP 94235	HD 178085	7.0	G1V	61.3	100.	Bin (new)	nonsat, ADI, H	
TYC 6893-1391-1	CD-25-14224	7.8	K2V	55.1	160.		sat, ADI, H	ccs
TYC 5206-0915-1	BD-07-5533	8.2	K1IV	76.4	300.		sat, ADI, H	
TYC 5736-0649-1	BD-14-5534	8.0	G6V	86.4	30.		sat, ADI, H	ccs
HD 189285	BD-04-4987	8.0	G5	77.8	100.		sat, ADI, H	cc
HIP 98470	HD 189245	4.6	F7V	21.2	100.		sat, ADI, H	
TYC 5164-567-1	BD-03-4778	8.0		63.3	100.		sat, ADI, H	ccs
HIP 99273	HD 191089	6.1	F5V	52.2	16.		sat, ADI, H	
HD 199058	BD+08-4561	7.0	G5	66.2	100.	Bin (new)	nonsat, ADI, H	
HIP 105384	HD 203019	6.4	K5V	35.0	400.		sat, ADI, H	cc
HIP 105612	HD 202732	6.3	G5V	32.8	600.		sat, ADI, H	
HIP 107684	HD 207278	8.1	G7V	90.2	100.	Bin (new)	nonsat, ADI, H	
HIP 108422	HD 208233	6.9	G9IV	58.0	30.	Bin (known)	nonsat, ADI, H	
TYC 8004-0083-1	CD-40-14901	7.9	G5V	74.9	100.		sat, ADI, H	
HIP 114046	HD 217897	3.6	M2V	3.3	8000.		sat, ADI, H	
TYC 9338-2016-1	HD 220054	8.3	G8V	99.6	30.		sat, ADI, H	
TYC 9529-0340-1	CD-86-147	7.6	G8IV	68.8	30.		sat, ADI, H	
TYC 9339-2158-1	CD-69-2101	6.8	K3V	30.6	300.		sat, ADI, H	
TYC 6406-0180-1	HD 221545	7.7	K0V	58.0	200.		sat, ADI, H	
HIP 116910	HD 222575	7.8	G8V	63.7	100.		sat, ADI, H	

Table 6. Companion candidate characterization and identification (for multi-epoch observations).

Name-1	UT-Date	Candidate	Sep (mas)	PA (deg)	ΔH (mag)	Status	Comments
TYC 5839-0596-1	2009-11-24	none					SB2
TYC 0603-0461-1	2009-11-24	none					New binary (see Table 5)
HIP 3924	2009-11-22	none					SB2
HIP 6177	2010-07-31	cc-1	1566 ± 6	118.4 ± 0.2	7.1 ± 0.1		
	2011-07-28	cc-1	1565 ± 10	118.0 ± 0.4		C	White dwarf companion
HIP 8038	2010-07-31	none					New binary (see Table 5)
HIP 10602	2009-11-24	none					A few exposures
	2010-07-30	none					
HIP 11360	2009-11-23	none					
TYC 8484-1507-1	2010-07-31	none					Known (~8.6″) binary resolved by 2MASS
HIP 12394	2009-11-22	none					
HIP 13008	2011-09-29	cc-1	1710 ± 7	347.3 ± 0.2	6.9 ± 0.0	U	
HIP 14684	2010-07-30	cc-1	5454 ± 13	150.6 ± 0.1	10.7 ± 0.1	B	
	2011-12-23	cc-1	5274 ± 6	150.3 ± 0.1	11.1 ± 0.1	B	
TYC 8060-1673-1	2009-11-23	none					
HIP 19775	2009-11-22	none					
HIP 23316	2009-11-23	none					
HD 32981	2009-11-24	none					
BD-09-1108	2009-11-22	none					
HIP 25434	2010-02-17	cc-1	4944 ± 11	154.5 ± 0.1	11.4 ± 0.1	B	
	2010-12-05	cc-1	4937 ± 5	154.5 ± 0.1	12.0 ± 0.1	B	
	2012-11-21	cc-1	4947 ± 7	155.1 ± 0.1	11.1 ± 0.1	B	
TYC 9162-0698-1	2010-02-19	26					Electronic table
	2011-01-24	26 + 33				B+U	Electronic table
TYC 5346-132-1	2009-11-23	cc-1	6252 ± 16	1.8 ± 0.2	9.7 ± 0.1	B	
	2010-02-16	cc-1	6260 ± 9	1.7 ± 0.1	9.8 ± 0.1	B	
	2009-11-23	cc-2	6431 ± 16	0.2 ± 0.2	9.1 ± 0.1	B	
	2010-02-16	cc-2	6434 ± 9	0.0 ± 0.1	9.1 ± 0.1	B	
HIP 30261	2009-11-23	none					
TYC 7617-0549-1	2009-11-21	cc-1	1848 ± 16	299.6 ± 0.5	12.6 ± 0.1	B	
	2012-11-22	cc-1	1861 ± 8	298.6 ± 0.3	12.1 ± 0.1	B	
TYC 9181-0466-1	2010-02-19	none					New binary (see Table 5)
HIP 32235	2010-02-18	cc-1	5559 ± 12	340.3 ± 0.2	11.8 ± 0.1	B	
	2010-12-30	cc-1	5508 ± 6	339.8 ± 0.1	13.3 ± 0.2	B	
HIP 35564	2009-11-22	cc-1	1865 ± 20	304.2 ± 0.6	15.3 ± 0.3	B	RV var
	2011-01-31	cc-1	1852 ± 8	299.3 ± 0.2	14.4 ± 0.7	B	
	2009-11-22	cc-2	3301 ± 20	148.9 ± 0.3	12.4 ± 0.1	B	
	2010-02-16	cc-2	3365 ± 13	148.7 ± 0.2	12.1 ± 0.1	B	
	2011-01-31	cc-2	3465 ± 9	149.8 ± 0.2	11.9 ± 0.1	B	
	2009-11-22	cc-3	6722 ± 20	1.5 ± 0.2	14.4 ± 0.3	B	
	2010-02-16	cc-3	6660 ± 12	1.8 ± 0.2	14.0 ± 0.4	B	
	2011-01-31	cc-3	6581 ± 8	1.7 ± 0.1	13.7 ± 0.4	B	
TYC 8128-1946-1	2009-11-21	cc-1	5521 ± 17	178.2 ± 0.2	13.5 ± 0.1	B	
	2011-01-20	cc-1	5549 ± 12	178.1 ± 0.2	13.7 ± 0.2	B	
	2009-11-21	cc-2	8211 ± 17	6.3 ± 0.2	9.4 ± 0.1	B	
	2011-01-20	cc-2	8190 ± 12	6.3 ± 0.1	9.9 ± 0.1	B	
HIP 36414	2010-02-17	cc-1	8296 ± 21	305.0 ± 0.2	12.8 ± 0.7	B	SB, RV var
	2011-01-31	cc-1	8241 ± 16	304.5 ± 0.1	13.5 ± 0.2	B	
	2010-02-17	cc-2	7076 ± 19	359.2 ± 0.2	13.6 ± 0.2	U	
HIP 36948	2010-02-16	cc-1	3485 ± 21	327.1 ± 0.3	14.1 ± 0.2	B	The Moth[a]
	2010-02-16	cc-2	6272 ± 22	315.5 ± 0.2	13.6 ± 0.2	B	
	2010-02-16	cc-3	7217 ± 20	191.3 ± 0.2	13.3 ± 0.4	B	
	2010-02-16	cc-4	8116 ± 20	171.1 ± 0.2	14.1 ± 0.8	B	
	2010-02-16	cc-5	8206 ± 20	268.1 ± 0.2	10.1 ± 0.1	B	
HIP 37563	2010-02-18	none					

Notes. Target name and observing date are given, as well as the different sources identified with their relative position, and relative flux, and their identification status based on follow-up observations. Sources are indicated follows: stationary background contaminants (B; based on a comoving companion probability $P_{\mathrm{comoving},\chi^2} < 1\%$ and with a relative motion compatible with a background source); confirmed comoving companions (C; based on a stationary background contaminant probability $P_{\mathrm{BKG},\chi^2} < 1\%$ and a relative motion compatible with a comoving companion); and undefined (U; when observed at only one epoch or when not satisfying the first two classifications). [a] All background objects identified combining NaCo with HST data by Buenzli et al. (2010). [b] Known binary (Brandner et al. 1996). [c] Known binary (Köhler et al. 2000). [d] Known binary (Chauvin et al. 2010).

Table 6. continued.

Name-1	UT-Date	Nb Cand.	Sep (mas)	PA (deg)	ΔH (mag)	Status	Comments
HIP 37923	2010-02-18	cc-1	5439 ± 10	261.2 ± 0.2	12.6 ± 0.1	B	
	2011-01-01	cc-1	5439 ± 8	259.8 ± 0.1	12.7 ± 0.1	B	
	2010-02-18	cc-2	5834 ± 12	55.5 ± 0.1	14.0 ± 0.1	B	
	2011-01-01	cc-2	5765 ± 10	56.5 ± 0.1	14.2 ± 0.2	B	
	2010-02-18	cc-3	5997 ± 12	209.9 ± 0.1	12.4 ± 0.1	B	
	2011-01-01	cc-3	6098 ± 10	209.1 ± 0.1	12.7 ± 0.1	B	
	2010-02-18	cc-4	7070 ± 12	28.2 ± 0.1	14.1 ± 0.3	B	
	2011-01-01	cc-4	6947 ± 10	28.8 ± 0.1	14.4 ± 0.2	B	
	2010-02-18	cc-5	8076 ± 13	65.1 ± 0.1	9.1 ± 0.1	B	
	2011-01-01	cc-5	8029 ± 10	65.9 ± 0.1	9.6 ± 0.1	B	
	2010-02-18	cc-6	8677 ± 15	43.1 ± 0.1	13.8 ± 0.2	U	
TYC 8927-3620-1	2010-02-19	none					New binary (see Table 5) Third component at ~4.8″ resolved by 2MASS
HIP 46634	2009-11-24	none					
HIP 47646	2010-02-18	none					
TWA-21	2010-02-18	cc-1	2353 ± 11	30.9 ± 0.3	13.8 ± 0.3	B	
	2011-01-13	cc-1	2339 ± 7	31.5 ± 0.2	14.2 ± 0.4	B	
	2010-02-18	cc-2	2508 ± 11	342.2 ± 0.3	13.9 ± 0.3	B	
	2011-01-13	cc-2	2489 ± 7	342.7 ± 0.2	14.2 ± 0.3	B	
	2010-02-18	cc-3	3152 ± 11	67.6 ± 0.2	12.2 ± 0.1	B	
	2011-01-13	cc-3	3178 ± 7	68.1 ± 0.2	12.8 ± 0.1	B	
	2010-02-18	cc-4	4968 ± 11	94.0 ± 0.2	13.4 ± 0.2	B	
	2011-01-13	cc-4	5003 ± 6	94.1 ± 0.1	14.0 ± 0.3	B	
	2010-02-18	cc-5	5231 ± 12	241.6 ± 0.2	8.9 ± 0.1	B	
	2011-01-13	cc-5	5210 ± 8	241.2 ± 0.1	9.4 ± 0.1	B	
	2010-02-18	cc-6	5355 ± 12	71.1 ± 0.2	11.7 ± 0.1	B	
	2011-01-13	cc-6	5387 ± 7	71.3 ± 0.1	12.4 ± 0.1	B	
	2010-02-18	cc-7	5602 ± 12	24.6 ± 0.1	9.1 ± 0.1	B	
	2011-01-13	cc-7	5599 ± 8	25.0 ± 0.1	9.7 ± 0.1	B	
	2010-02-18	cc-8	5712 ± 12	27.8 ± 0.1	12.7 ± 0.1	B	
	2011-01-13	cc-8	5717 ± 9	28.0 ± 0.1	13.2 ± 0.1	B	
	2010-02-18	cc-9	5801 ± 12	245.6 ± 0.1	10.2 ± 0.1	B	
	2011-01-13	cc-9	5776 ± 8	245.3 ± 0.1	10.7 ± 0.1	B	
	2010-02-18	cc-10	5833 ± 11	102.6 ± 0.2	13.4 ± 0.2	B	
	2011-01-13	cc-10	5879 ± 7	102.6 ± 0.1	14.0 ± 0.2	B	
	2010-02-18	cc-11	6097 ± 12	107.7 ± 0.1	12.6 ± 0.1	B	
	2011-01-13	cc-11	6138 ± 7	107.7 ± 0.1	13.3 ± 0.1	B	
	2010-02-18	cc-12	6951 ± 13	147.5 ± 0.1	13.6 ± 0.2	B	
	2011-01-13	cc-12	6990 ± 10	147.4 ± 0.1	14.4 ± 0.4	B	
	2010-02-18	cc-13	3369 ± 11	165.3 ± 0.2	14.3 ± 0.3	U	
	2010-02-18	cc-14	5948 ± 13	228.5 ± 0.1	15.0 ± 0.4	U	
	2011-01-13	cc-15	7049 ± 7	9.4 ± 0.1	12.9 ± 0.1	U	
TYC 7188-0575-1	2010-02-16	cc-1	4238 ± 15	296.5 ± 0.2	15.2 ± 0.4	B	SB2
	2011-01-27	cc-1	4148 ± 12	297.5 ± 0.2	14.8 ± 0.4	B	
	2010-02-16	cc-2	4741 ± 15	61.7 ± 0.2	11.6 ± 0.1	B	
	2011-01-27	cc-2	4843 ± 12	62.2 ± 0.2	11.4 ± 0.1	B	
	2010-02-16	cc-3	5329 ± 15	186.0 ± 0.2	11.9 ± 0.1	B	
	2011-01-27	cc-3	5303 ± 11	185.1 ± 0.2	11.8 ± 0.1	B	
	2010-02-16	cc-4	7391 ± 15	279.5 ± 0.2	13.2 ± 0.2	B	
	2011-01-27	cc-4	7282 ± 11	279.8 ± 0.1	13.1 ± 0.2	B	
	2010-02-16	cc-5	8020 ± 15	5.1 ± 0.2	11.6 ± 0.1	B	
	2011-01-27	cc-5	8058 ± 11	5.8 ± 0.1	11.7 ± 0.1	B	
TYC 6069-1214-1	2010-02-17	none					
TYC 7722-0207-1	2010-02-17	cc-1	3981 ± 11	33.5 ± 0.2	11.7 ± 0.1	B	
	2011-01-29	cc-1	3978 ± 6	35.0 ± 0.1	11.5 ± 0.1	B	
	2010-02-17	cc-2	4369 ± 12	228.1 ± 0.2	7.3 ± 0.1	B	
	2011-01-29	cc-2	4355 ± 7	226.9 ± 0.1	7.1 ± 0.1	B	
	2010-02-17	cc-3	8516 ± 11	105.2 ± 0.1	9.4 ± 0.1	B	
	2011-01-29	cc-3	8602 ± 6	105.4 ± 0.1	9.1 ± 0.1	B	
	2010-02-17	cc-4	1742 ± 10	329.8 ± 0.3	13.9 ± 0.5	U	
	2011-01-29	cc-5	7958 ± 11	317.3 ± 0.1	10.1 ± 0.1	U	
	2011-01-29	cc-6	7988 ± 11	42.2 ± 0.1	12.4 ± 0.1	U	

Table 6. continued.

Name-1	UT-Date	Nb Cand.	Sep (mas)	PA (deg)	ΔH (mag)	Status	Comments
TYC 7743-1091-1	2010-02-19	none					
HIP 58240	2010-02-16	cc-1	5761 ± 21	179.6 ± 0.2	13.0 ± 0.2	B	
	2011-01-29	cc-1	5770 ± 5	178.1 ± 0.1	12.9 ± 0.1	B	
TYC 9231-1566-1	2010-02-19	none					New binary (see Table 5)
TYC 8979-1683-1	2010-02-18	54(+16)					Electronic table
	2011-05-11	54				B(+U)	Electronic table
TYC 8989-0583-1	2010-02-18	none					New binary (see Table 5)
	2010-06-16	none					
TYC 9245-0617-1	2010-02-18	cc-1	3771 ± 10	32.2 ± 0.2	9.5 ± 0.1	B	
	2013-02-11	cc-1	3860 ± 5	33.2 ± 0.1	9.1 ± 0.1	B	
	2010-02-18	cc-2	3942 ± 10	119.4 ± 0.2	5.9 ± 0.1	B	
	2011-04-04	cc-2	3974 ± 10	118.9 ± 0.2	6.0 ± 0.1	B	
	2013-02-11	cc-2	4015 ± 5	118.4 ± 0.1	5.8 ± 0.1	B	
	2010-02-18	cc-3	6544 ± 9	183.4 ± 0.1	10.9 ± 0.1	B	
	2013-02-11	cc-3	6517 ± 3	182.4 ± 0.1	10.9 ± 0.3	B	
	2010-02-18	cc-4	7448 ± 11	241.0 ± 0.1	10.2 ± 0.1	B	
	2013-02-11	cc-4	7342 ± 8	241.0 ± 0.1	10.2 ± 0.2	B	
	2010-02-18	cc-5	4590 ± 10	306.1 ± 0.1	12.8 ± 0.1	U	
	2010-02-18	cc-6	5603 ± 9	263.3 ± 0.1	14.5 ± 0.3	U	
	2010-02-18	cc-7	5887 ± 9	179.7 ± 0.1	12.2 ± 0.1	U	
	2010-02-18	cc-8	6149 ± 10	251.4 ± 0.1	13.3 ± 0.2	U	
	2010-02-18	cc-9	7432 ± 12	146.0 ± 0.1	11.9 ± 0.1	U	
	2010-02-18	cc-10	8529 ± 10	73.1 ± 0.1	12.9 ± 0.2	U	
HIP 63862	2010-02-18	cc-1	4231 ± 16	28.0 ± 0.2	12.9 ± 0.1	B	
	2011-07-02	cc-1	4315 ± 5	30.7 ± 0.1	13.1 ± 0.1	B	
	2010-02-18	cc-2	5536 ± 17	206.7 ± 0.2	12.8 ± 0.1	B	
	2011-07-02	cc-2	5478 ± 5	204.8 ± 0.1	13.3 ± 0.1	B	
	2011-07-02	cc-3	7186 ± 5	160.1 ± 0.1	14.1 ± 0.2	U	
	2011-07-02	cc-4	8169 ± 10	142.8 ± 0.1	12.7 ± 0.1	U	
TYC 7796-2110-1	2010-02-16	cc-1	3264 ± 15	127.0 ± 0.3	11.3 ± 0.1	B	
	2011-05-11	cc-1	3306 ± 4	126.3 ± 0.1	11.1 ± 0.3	B	
	2013-03-22	cc-1	3314 ± 9	125.2 ± 0.2	11.2 ± 0.1	B	
	2010-02-16	cc-2	3990 ± 16	141.6 ± 0.2	8.7 ± 0.1	B	
	2011-05-11	cc-2	4018 ± 5	141.1 ± 0.1	8.8 ± 0.1	B	
	2013-03-22	cc-2	4034 ± 9	140.3 ± 0.1	8.7 ± 0.1	B	
	2010-02-16	cc-3	4111 ± 15	109.7 ± 0.2	13.5 ± 0.2	B	
	2013-03-22	cc-3	4190 ± 8	108.5 ± 0.1	13.6 ± 0.3	B	
	2010-02-16	cc-4	5231 ± 16	151.6 ± 0.2	13.2 ± 0.1	B	
	2013-03-22	cc-4	5194 ± 10	150.7 ± 0.1	13.3 ± 0.2	B	
	2010-02-16	cc-5	6324 ± 17	214.1 ± 0.2	12.5 ± 0.1	B	
	2013-03-22	cc-5	6211 ± 11	214.0 ± 0.1	12.4 ± 0.1	B	
	2010-02-16	cc-6	7111 ± 16	62.6 ± 0.2	10.8 ± 0.1	B	
	2011-05-11	cc-6	7145 ± 7	62.8 ± 0.1	11.1 ± 0.3	B	
	2013-03-22	cc-6	7240 ± 10	62.8 ± 0.1	10.8 ± 0.1	B	
	2010-02-16	cc-7	8743 ± 18	48.5 ± 0.1	14.0 ± 0.4	U	
TYC 9010-1272-1	2010-02-18	none					New binary (see Table 5)
HIP 70351	2010-02-17	cc-1	2971 ± 10	258.4 ± 0.2	14.7 ± 0.4	U	
	2010-02-17	cc-2	4664 ± 11	288.7 ± 0.2	11.4 ± 0.1	U	
	2010-02-17	cc-3	4973 ± 10	4.0 ± 0.2	13.9 ± 0.2	U	
	2010-02-17	cc-4	6572 ± 10	262.2 ± 0.1	13.5 ± 0.1	U	
	2010-02-17	cc-5	6615 ± 13	235.8 ± 0.1	13.0 ± 0.1	U	
	2010-02-17	cc-6	6820 ± 13	145.7 ± 0.1	11.0 ± 0.1	U	
	2010-02-17	cc-7	7266 ± 12	118.2 ± 0.1	12.9 ± 0.1	U	
HIP 71908	2010-02-16	cc-1	6404 ± 16	28.4 ± 0.2	16.3 ± 0.4	U	
HIP 71933	2010-06-15	cc-1	4934 ± 9	12.6 ± 0.1	10.0 ± 0.1	B	
	2011-04-06	cc-1	4952 ± 2	12.8 ± 0.1	9.4 ± 0.1	B	
	2013-02-23	cc-1	5031 ± 3	13.1 ± 0.1	10.0 ± 0.1	B	
	2010-06-15	cc-2	5864 ± 11	54.1 ± 0.1	11.3 ± 0.1	B	
	2013-02-23	cc-2	5958 ± 7	54.0 ± 0.1	11.3 ± 0.1	B	

Table 6. continued.

Name-1	UT-Date	Nb Cand.	Sep (mas)	PA (deg)	ΔH (mag)	Status	Comments
HIP 71933	2010-06-15	cc-3	7987 ± 9	12.5 ± 0.1	10.4 ± 0.1	B	
	2011-04-06	cc-3	8006 ± 3	12.8 ± 0.1	9.8 ± 0.2	B	
	2013-02-23	cc-3	8096 ± 4	13.1 ± 0.1	10.4 ± 0.1	B	
	2010-06-15	cc-4	9258 ± 12	205.1 ± 0.1	9.2 ± 0.1	B	
	2013-02-23	cc-4	9127 ± 8	205.1 ± 0.1	9.5 ± 0.1	B	
	2010-06-15	cc-5	5434 ± 10	22.6 ± 0.1	13.3 ± 0.1	U	
	2010-06-15	cc-6	6963 ± 10	107.8 ± 0.1	13.9 ± 0.2	U	
	2010-06-15	cc-7	7158 ± 12	130.1 ± 0.1	12.4 ± 0.1	U	
	2010-06-15	cc-8	7968 ± 11	202.0 ± 0.1	13.9 ± 0.3	U	
	2010-06-15	cc-9	8756 ± 9	12.5 ± 0.1	12.9 ± 0.2	U	
HIP 72399	2011-05-27	none					SB1, RV var
TYC 7835-2569-1	2011-05-11	none					SB2 + Known binary[b]
HIP 76829	2010-06-15	cc-1	2393 ± 4	46.8 ± 0.1	15.0 ± 0.4	B	
	2011-06-27	cc-1	2705 ± 9	45.7 ± 0.2	14.5 ± 0.5	B	
	2010-06-15	cc-2	6368 ± 6	111.7 ± 0.1	14.8 ± 0.3	B	
	2011-06-27	cc-2	6434 ± 10	109.1 ± 0.1	14.2 ± 0.3	B	
	2010-06-15	cc-3	4481 ± 6	310.5 ± 0.1	16.3 ± 0.6	U	
	2010-06-15	cc-4	5272 ± 3	272.4 ± 0.1	16.3 ± 0.4	U	
	2010-06-15	cc-5	5900 ± 3	91.3 ± 0.1	16.2 ± 0.4	U	
	2010-06-15	cc-6	8618 ± 11	142.8 ± 0.1	15.2 ± 0.4	U	
TYC 6781-0415-1	2011-07-20	none					
TYC 6786-0811-1	2010-07-29	none					Known binary[c]
HIP 78747	2010-07-29	cc-1	3892 ± 2	0.6 ± 0.1	11.9 ± 0.1	B	
	2011-06-28	cc-1	3990 ± 4	2.2 ± 0.1	12.0 ± 0.1	B	
	2010-07-29	cc-2	6154 ± 5	292.2 ± 0.1	12.8 ± 0.1	B	
	2011-06-28	cc-2	6110 ± 6	293.5 ± 0.1	13.0 ± 0.2	B	
	2010-07-29	cc-3	6633 ± 8	53.9 ± 0.1	12.7 ± 0.1	B	
	2011-06-28	cc-3	6788 ± 9	53.9 ± 0.1	12.8 ± 0.2	B	
	2010-07-29	cc-4	5508 ± 6	59.0 ± 0.1	14.6 ± 0.2	U	
	2010-07-29	cc-5	5949 ± 2	1.1 ± 0.1	14.7 ± 0.3	U	
	2010-07-29	cc-6	7557 ± 5	200.8 ± 0.1	14.0 ± 0.2	U	
	2011-06-28	cc-7	7419 ± 5	255.3 ± 0.1	13.2 ± 0.2	U	
TYC 6209-0769-1	2011-08-19	cc-1	5473 ± 3	198.6 ± 0.1	8.2 ± 0.1	U	
HIP 79958	2011-06-27	cc-1	3583 ± 4	29.3 ± 0.1	11.7 ± 0.3	U	
	2011-06-27	cc-2	3689 ± 1	88.8 ± 0.1	9.4 ± 0.1	U	
	2011-06-27	cc-3	4120 ± 2	281.1 ± 0.1	10.2 ± 0.1	U	
	2011-06-27	cc-4	4633 ± 4	151.3 ± 0.1	11.5 ± 0.2	U	
	2011-06-27	cc-5	5986 ± 2	169.4 ± 0.1	10.9 ± 0.1	U	
	2011-06-27	cc-6	6195 ± 1	177.4 ± 0.1	10.6 ± 0.1	U	
	2011-06-27	cc-7	7628 ± 2	350.9 ± 0.1	11.3 ± 0.3	U	
HIP 80290	2011-08-08	cc-1	2688 ± 1	184.6 ± 0.1	8.5 ± 0.1	B	
	2012-08-12	cc-1	2665 ± 7	184.3 ± 0.2	9.1 ± 0.1	B	
	2011-08-08	cc-2	3340 ± 1	257.5 ± 0.1	1.9 ± 0.1	C	
	2012-08-12	cc-2	3335 ± 8	257.6 ± 0.2	2.6 ± 0.1	C	New binary (see Table 5)
	2011-08-08	cc-3	7425 ± 9	143.6 ± 0.1	6.9 ± 0.1	B	
	2012-08-12	cc-3	7417 ± 12	143.4 ± 0.1	7.6 ± 0.1	B	
	2012-08-12	cc-4	2097 ± 8	34.3 ± 0.2	12.4 ± 0.3	U	
	2012-08-12	cc-5	2245 ± 8	291.3 ± 0.2	11.1 ± 0.1	U	
	2012-08-12	cc-6	6186 ± 8	94.6 ± 0.1	12.0 ± 0.1	U	
	2012-08-12	cc-7	8629 ± 11	298.8 ± 0.1	11.0 ± 0.1	U	
HIP 80758	2010-07-29	cc-1	2210 ± 3	163.6 ± 0.1	12.9 ± 0.1	B	
	2011-05-11	cc-1	2171 ± 7	163.3 ± 0.2	12.2 ± 0.2	B	
	2010-07-29	cc-2	2221 ± 4	241.1 ± 0.1	12.5 ± 0.1	B	
	2011-05-11	cc-2	2192 ± 7	242.1 ± 0.2	11.8 ± 0.2	B	
	2010-07-29	cc-3	2413 ± 4	321.1 ± 0.1	12.8 ± 0.1	B	
	2011-05-11	cc-3	2455 ± 7	321.7 ± 0.2	12.3 ± 0.2	B	
	2010-07-29	cc-4	4686 ± 6	236.1 ± 0.1	11.5 ± 0.1	B	
	2011-05-11	cc-4	4651 ± 8	236.6 ± 0.1	10.9 ± 0.1	B	
	2010-07-29	cc-5	5228 ± 7	304.1 ± 0.1	12.7 ± 0.1	B	
	2011-05-11	cc-5	5256 ± 9	304.6 ± 0.1	12.1 ± 0.1	B	
	2010-07-29	cc-6	5229 ± 5	70.3 ± 0.1	13.9 ± 0.2	B	
	2011-05-11	cc-6	5215 ± 8	69.9 ± 0.1	12.9 ± 0.2	B	

Table 6. continued.

Name-1	UT-Date	Nb Cand.	Sep (mas)	PA (deg)	ΔH (mag)	Status	Comments
HIP 80758	2010-07-29	cc-7	5441 ± 5	108.0 ± 0.1	11.9 ± 0.1	B	
	2011-05-11	cc-7	5418 ± 7	107.7 ± 0.1	10.9 ± 0.1	B	
	2010-07-29	cc-8	5489 ± 6	25.2 ± 0.1	10.2 ± 0.1	B	
	2011-05-11	cc-8	5523 ± 8	24.8 ± 0.1	9.6 ± 0.1	B	
	2010-07-29	cc-9	7495 ± 4	79.1 ± 0.1	6.7 ± 0.1	B	
	2011-05-11	cc-9	7472 ± 7	78.7 ± 0.1	5.7 ± 0.1	B	
	2010-07-29	cc-10	7925 ± 3	265.4 ± 0.1	12.7 ± 0.2	B	
	2011-05-11	cc-10	7897 ± 7	265.5 ± 0.1	12.4 ± 0.3	B	
	2010-07-29	cc-11	3005 ± 4	22.0 ± 0.1	14.4 ± 0.3	U	
TYC 6818-1336-1	2011-07-20	cc-1	3382 ± 10	302.7 ± 0.2	7.3 ± 0.1	U	
	2011-07-20	cc-2	5824 ± 10	291.7 ± 0.1	5.5 ± 0.1	U	
	2011-07-20	cc-3	8914 ± 14	52.1 ± 0.1	2.8 ± 0.1	U	
TYC 6815-0084-1	2013-06-02	none					SB2?
TYC 6815-0874-1	2012-08-13	cc-1	2094 ± 16	229.6 ± 0.4	12.2 ± 0.2	U	
	2012-08-13	cc-2	2224 ± 16	333.4 ± 0.4	11.9 ± 0.2	U	
	2012-08-13	cc-3	2713 ± 16	280.7 ± 0.4	12.8 ± 0.2	U	
	2012-08-13	cc-4	2754 ± 16	12.8 ± 0.3	11.1 ± 0.1	U	
	2012-08-13	cc-5	3801 ± 16	171.0 ± 0.3	9.6 ± 0.1	U	
	2012-08-13	cc-6	4035 ± 17	36.9 ± 0.2	12.1 ± 0.1	U	
	2012-08-13	cc-7	4940 ± 17	164.2 ± 0.2	13.2 ± 0.2	U	
	2012-08-13	cc-8	6046 ± 17	285.5 ± 0.2	12.9 ± 0.2	U	
	2012-08-13	cc-9	6569 ± 17	22.6 ± 0.2	13.1 ± 0.2	U	
	2012-08-13	cc-10	8354 ± 19	306.1 ± 0.1	12.4 ± 0.2	U	
	2012-08-13	cc-11	9053 ± 19	125.0 ± 0.1	12.0 ± 0.1	U	
TYC 7362-0724-1	2010-06-16	57(+211)					Electronic table
	2011-05-11	57				B(+U)	Electronic table
TYC 8728-2262-1	2011-08-25	cc-1	2821 ± 12	254.8 ± 0.3	9.1 ± 0.1	U	
	2011-08-25	cc-2	4449 ± 13	27.5 ± 0.2	11.4 ± 0.1	U	
	2011-08-25	cc-3	6232 ± 14	130.2 ± 0.1	12.1 ± 0.2	U	
	2011-08-25	cc-4	6399 ± 12	99.3 ± 0.2	6.3 ± 0.0	U	
	2011-08-25	cc-5	6883 ± 12	166.3 ± 0.1	12.4 ± 0.1	U	
HIP 86672	2010-06-16	261					Electronic table
	2011-08-25	none					
	2013-04-25	80(+181)				B(+U)	Electronic table
HIP 89829	2011-06-13	99					Electronic table
	2012-08-09	29(+70)				B(+U)	Electronic table
HIP 93375	2010-06-14	cc-1	3208 ± 11	121.6 ± 0.2	13.8 ± 0.2	B	
	2011-05-30	cc-1	3175 ± 9	120.5 ± 0.2	13.6 ± 0.2	B	
	2010-06-14	cc-2	4261 ± 10	9.2 ± 0.2	13.7 ± 0.2	B	
	2011-05-30	cc-2	4335 ± 8	9.0 ± 0.2	13.4 ± 0.2	B	
	2010-06-14	cc-3	4595 ± 10	264.5 ± 0.2	12.5 ± 0.1	B	
	2011-05-30	cc-3	4591 ± 8	265.7 ± 0.2	12.8 ± 0.1	B	
	2010-06-14	cc-4	4822 ± 12	139.6 ± 0.1	11.4 ± 0.1	B	
	2011-05-30	cc-4	4754 ± 10	138.9 ± 0.1	11.5 ± 0.1	B	
	2010-06-14	cc-5	5308 ± 10	173.7 ± 0.2	13.7 ± 0.2	B	
	2011-05-30	cc-5	5218 ± 8	173.6 ± 0.1	13.5 ± 0.1	B	
	2010-06-14	cc-6	5354 ± 10	176.9 ± 0.2	14.0 ± 0.2	B	
	2011-05-30	cc-6	5283 ± 8	177.1 ± 0.1	14.0 ± 0.2	B	
	2010-06-14	cc-7	6095 ± 10	274.5 ± 0.1	12.0 ± 0.1	B	
	2011-05-30	cc-7	6104 ± 8	275.2 ± 0.1	12.7 ± 0.1	B	
	2010-06-14	cc-8	6848 ± 10	185.1 ± 0.1	12.4 ± 0.1	B	
	2011-05-30	cc-8	6763 ± 8	184.9 ± 0.1	11.6 ± 0.1	B	
	2010-06-14	cc-9	6942 ± 12	153.9 ± 0.1	12.4 ± 0.1	B	
	2011-05-30	cc-9	6856 ± 10	154.2 ± 0.1	11.6 ± 0.1	B	
	2010-06-14	cc-10	7089 ± 14	46.6 ± 0.1	12.9 ± 0.1	B	
	2011-05-30	cc-10	7143 ± 12	45.8 ± 0.1	13.5 ± 0.2	B	
	2010-06-14	cc-11	7502 ± 13	116.6 ± 0.1	11.1 ± 0.1	U	
	2010-06-14	cc-12	7512 ± 12	115.1 ± 0.1	12.6 ± 0.1	U	
	2011-05-30	cc-13	4157 ± 9	237.0 ± 0.1	14.1 ± 0.2	U	
	2011-05-30	cc-14	5917 ± 8	262.2 ± 0.1	14.4 ± 0.3	U	
	2011-05-30	cc-15	9234 ± 14	322.3 ± 0.1	11.5 ± 0.1	U	

Table 6. continued.

Name-1	UT-Date	Nb Cand.	Sep (mas)	PA (deg)	ΔH (mag)	Status	Comments
HIP 94235	2010-07-30	none					New binary (see Table 6)
TYC 6893-1391-1	2011-06-08	cc-1	3289 ± 4	229.6 ± 0.1	11.2 ± 0.2	U	
	2011-06-08	cc-2	3373 ± 1	256.6 ± 0.1	11.8 ± 0.3	U	
	2011-06-08	cc-3	5761 ± 7	224.5 ± 0.1	6.8 ± 0.0	U	
TYC 5206-0915-1	2010-07-30	none					
TYC 5736-0649-1	2011-08-18	cc-1	4360 ± 6	206.3 ± 0.1	9.8 ± 0.1	U	
	2011-08-18	cc-2	6130 ± 8	306.9 ± 0.1	10.6 ± 0.1	U	
HD 189285	2011-08-20	cc-1	4519 ± 4	24.9 ± 0.1	9.5 ± 0.1	U	
HIP 98470	2010-06-15	none					
TYC 5164-567-1	2011-07-29	cc-1	2632 ± 3	207.5 ± 0.1	3.3 ± 0.0	U	
	2011-07-29	cc-2	4421 ± 5	56.8 ± 0.1	11.2 ± 0.1	U	
	2011-07-29	cc-3	5674 ± 7	229.3 ± 0.1	8.6 ± 0.1	U	
	2011-07-29	cc-4	7254 ± 9	139.8 ± 0.1	9.8 ± 0.1	U	
HIP 99273	2010-07-31	none					
HD 199058	2010-06-15	none					New binary (see Table 6)
HIP 105384	2010-07-31	none					
	2011-06-08	cc-1	7038 ± 7	24.5 ± 0.1	14.1 ± 0.2	U	
HIP 105612	2010-07-31	none					
HIP 107684	2010-06-15	none					New binary (see Table 6)
HIP 108422	2010-07-30	none					Known binary[d]
TYC 8004-0083-1	2010-06-15	none					
HIP 114046	2010-06-15	none					
TYC 9338-2016-1	2009-11-23	none					
	2010-07-30	none					
TYC 9529-0340-1	2010-07-31	none					
TYC 9339-2158-1	2010-07-31	none					
TYC 6406-0180-1	2010-07-30	none					
HIP 116910	2009-11-22	none					